The Libyan Academy
Tripoli – Libya

School of Applied Sciences and Engineering
Department of Electrical and Computer Engineering

Design of an Antenna for Ground Penetrating Radar (GPR)

By:
Zayed Mohammed Habib

A Dissertation Submitted to the Department of Electrical and Computer Engineering in Conformity with the Department Requirements as a Partial Fulfillment for the Degree of Master of Engineering Sciences.

Supervised by:
Dr. Said Ibrahim Elkhetali

March 2014

Acknowledgment

First of all I would like to thank ALAH that give me the ability and support for achieve and accomplish this work.

I would also like to express my deepest appreciation and gratitude to my supervisor Dr. SAID IBRAHIM ELKHTALI for his advice, patience and invaluable guidance throughout my research.

Also I would like to thank my colleague Eng. OMAR S. ELSHIBANI for his help in doing part two experiments .

I would like to thank all my teachers in the department of electrical and computer engineering and everybody help me.

Last but not least, I would like to thank my family for all support and the encouragement that given for me.

ABSTRACT

One the objectives of this thesis is to investigate the performance of a bowtie antenna in both frequency and time domains for using it in the Ground Penetrating Radar (GPR) in field of landmines detection. The other objective is studying the effect of soil on the delectability of landmines and a Vector Network Analyzer (VNA) is used a GPR for this purpose.

The principle analytical tool utilized for studying the antenna in this study is the Finite Difference Time Domain method (FDTD) using three-dimensional full wave electromagnetic analysis software version 6.3 by Remcom.

The optimize of GPR antenna is always a question of trade-offs between specifications related to the targeted application, in this work trade-off was between resolution i.e. bandwidth and depth of penetration also between antenna efficiency and low time ringing. Such antenna must be able to transmit the signal with little distortion and less ringing in order to avoid masking of the target reflection. This requires an antenna with broadband properties and very short impulse response.

Resistive loaded bowtie antenna is presented to minimize late time ringing, also a padding shield is used to improve antenna bandwidth and concentrating most of antenna radiation into ground and reduce the influence of external signals on antenna. The effect of ground on bowtie antenna characteristics and capability of the GPR system to detect buried targets is simulated and studied .

In the second part two horn antennas connected with VNA is used as a GPR system. The performance of GPR system is studied over three types of soils.

TABLE OF CONTENTS

TABLE OF FIGURES

TABLE OF TABLES

Table Page

LIST OF ABBERVIATIONS

AP	Anti-Personal
A/S	Acoustic-to-Seismic
AT	Anti-Tank
BW	Bandwidth
CW	Continuous Wave
EIT	Electrical Impedance Tomography
EM	Electro-Magnetic
EMI	Electro-Magnetic Induction
EVD	Explosive Vapor Detection
FDTD	Finite Difference Time Domain
GPR	Ground Penetrating Radar
HPBW	Half Power Beam Width
PEC	Perfect Electrical Conductor
Pptr	Part per trillion
RDX	Royal Demolition Explosive
SFCW	Stepped Frequency Continuous Wave
SPR	Surface Penetrating Radar
TNT	Tri-Nitro-Toluene
TWTT	Two Way Travelling Time
UWB	Ultra Wide Band
VNA	Vector Network Analyzer
VSWR	Voltage Standing Wave Ratio

Chapter 1

Introduction

1-1 Introduction

Landmines are causing enormous humanitarian and economic problems in many countries all over the world. According to UN, there are up to 110 million landmines in nearly 70 countries that need to be cleared **[1]**. Most of the victims are innocent children and women. However, landmine detection and clearance have turned out to be an extremely challenging problem.

Landmines are prominent weapons, and they are harmful and effective, yet cheap, easy to make and lay. On average, the cost to produce a single mine is $3 USD (anti-personnel) to $75 USD (anti-tank), and they can be laid quickly in great quantities by unskilled personnel. In contrast, removal must be done by highly skilled personnel, and may cost, on average, $300 to $500 USD per mine. Even with highly trained deminers, UN statistics indicate a loss of one or two deminers per 1000 mines removed **[2]**.

Ground Penetrating Radar (GPR) is an electromagnetic techniques designed primarily for the location of objects or interfaces buried beneath the earth's surface or located within a non-visually structure. GPR is one of a number of technologies that has been used to improving the efficiency of landmine clearance operations.

One of the most important hardware components for the performance of a GPR is the antenna. The antenna must satisfy different standards than in usual radar antennas. Most GPR systems operate in the vicinity of the ground. Therefore, the important parameters determining the system performance, such as antenna beamwidth, and bandwidth, depend on the properties of the ground. The optimal antenna design must provide steady performance for different ground types and weather conditions.

1-2 Objective of Thesis

The main objective of this thesis is to investigate and optimize a bowtie antenna for impulse ground penetrating radar used to detect land mines and using two horn antennas connected with VNA is used as a GPR system.

1-3 Thesis Outlines

This thesis consists of seven chapters as follows:

Chapter 1 Introduction: gives a brief introduction of world landmines problems, objective of thesis and outlines of thesis.

Chapter 2 Landmine Detection Techniques: gives a brief introduction of landmines detection techniques and their operating principles, strengths and limitations.

Chapter 3 Electromagnetic wave propagation in materials: provides information on the electrical properties of soils (relative permittivity, conductivity and permeability) and a brief literature review on electromagnetic wave propagation in dielectric materials and the effect of water content on wave propagation.

Chapter 4 Ground Penetrating Radar: presents a more detailed definition for GPR, working principle, applications, types, GPR system (main components), antenna parameters and GPR antenna requirements, also gives a brief definition for bowtie antenna.

Chapter 5 FDTD simulation for GPR antenna: gives a brief introduction of FDTD method and presents a three dimension simulation of bowtie antenna in free space and over two types of grounds by using Remcom xFDTD package software (*Three-dimensional full wave electromagnetic analysis software version 6.3*)

Chapter 6 Using VNA with horn antenna as a GPR system: gives a brief introduction of general-purpose VNA and utilize it with horn antenna to works as a GPR system and check the performance of GPR system over three types of soils, estimating the velocity of EM wave in sand soil, dielectric constant of clay soil and try to detect metal targets in both soils by measuring the transmission coefficient S_{21} between two antennas.

Chapter 7 Conclusion and future work concludes and summaries of important points in the thesis and recommendations for future work.

Chapter 2

Landmine Detection Techniques

2-1 Landmines Types and Sizes

Although there are approximately 600 different types of landmines as shown in Figure (2-1), they can be divided into two main categories, Anti-Personnel (AP) and Anti-tank (AT) **[3]** as shown in Figures (2-2) and (2-3). Since the First World War, has proved to be an effective military weapon. They deny an enemy access to areas, and can deflect, delay and/or destroy enemy forces. They can also serve as a nuisance to disrupt lines of supply and demoralize opposing forces.

Figure (2-1) Different Types of Landmines

Figure (2-2) TAB-1 Brazilian Low-Metal AP Landmine

Figure (2-3) 72 SP Chinese Metallic AT Landmine

Mines are produced in different shapes, sizes, explosive intensity and fusing. Both AP and AT landmines come in all shapes and sizes, and can be encased in metal, plastic, wood, ceramics or nothing at all. Their fusing mechanism are also different, such as simple pressure triggers, trip wires, tilt rods, acoustic and seismic fuses, remote sensors, or even light or magnetic-influenced fuses. They can be embedded in a field cluttered with various materials and objects, buried underground at various depths, scattered on the surface, planted within buildings and on the roads, or covered by plant overgrowth.

AP mines are typically shaped in the form of a disk, a box or a cylinder, with diameters from 2 to 12.5 cm, length from 5 to 10 cm, and can weigh as little as 30 g Tri-Nitro-

Toluene (TNT), Royal Demolition Explosive (RDX), and mixture of TNT and RDX (Comp B) are the common types of explosives used. AP's are usually shallow buried, at a range from flush to the surface to a maximum depth of about 5 cm; as they do reduced damage if buried any deeper.

AT mines often have the shape of truncated cylinders or squares with round corners, with a dimension from 15 to 30 cm, and a thickness of 5 to 9 cm. The explosive material is typically TNT, Comp B, or RDX. AT's are buried at various depths from flush to the surface to greater than 15 cm.

2-2 Landmine Detection Techniques

There are many researches in physical, chemical, and biological sciences are studying and developing methods that could be used for landmine detection. New detection concepts involve searching for characteristics other than mine metal content. The techniques that exploit properties of the electromagnetic spectrum are being explored. In addition, research is under way to develop methods based on acoustics of the mine casing. Biological and chemical methods for detecting explosive vapors also are being explored, as are methods for detecting bulk explosives based on chemical properties. Research is being concerned many universities, government institutions, and private companies, with different projects in various stages of development. However, most of the technologies have not yet been field tested. This makes it virtually impossible to consider operating characteristics **[4].**

The performance of a landmine detection system depends on the types and depths of mines present, the environment in which the system is operated, and the human operator. For detectors that locate buried objects, such mine properties as size, shape, and metallic content substantially affect detector performance, as do the placements (depth and orientation) of the mines. Detectors that search for explosives can be sensitive to the type of explosive contained within the mine. Detector performance is also tied to persistent environmental attributes (such as soil type, terrain, vegetation, and clutter density) and transient atmospheric conditions (wind, humidity, soil moisture, and radio frequency or acoustic interference). So these techniques classified in way of its operating principle as the following:

- Electromagnetic Detection Techniques
- Acoustic/Seismic Techniques
- Explosive Vapor Detection Techniques
- Mechanical techniques

We will try in the next section of this chapter to give a brief idea for *Electromagnetic Detection Techniques*, its description, strengths and limitations.

2-3 Electromagnetic Detection Techniques

This kind of systems based on changes in the electromagnetic properties of the surface soil and shallow subsurface, and these systems include:

- Electromagnetic induction (metal detector)

-Electrical Impedance Tomography (EIT)

-X-Ray Backscatter

- Infrared/Hyper-spectral Systems

- Ground-Penetrating Radar (GPR**)**

These techniques will be described briefly in the following subsections.

2-3.1 Electromagnetic Induction (Metal Detector)

The metal detector is the most popular sensor to detect mines. It consists of a coil generating a magnetic field which may be disturbed by a metal object. The consequence is a higher power consumption or a change in the magnetic field induced into another coil as shown in Figure (2-4). Unfortunately this method is often unreliable or time consuming, because some mines have minimum metal to detect and is not recognizable within all kinds of metallic objects (metal clutter) on a former battle field **[5]**.

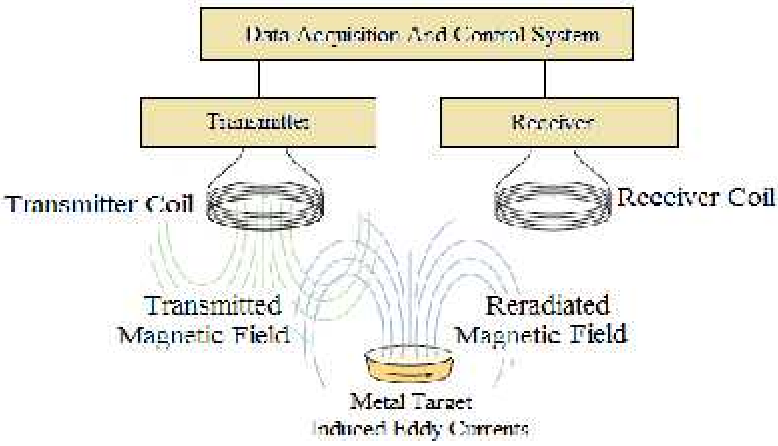

Figure (2-4) Simplified Diagram of the Basic EMI Technique

2-3.2 Electrical Impedance Tomography (EIT)

EIT uses electrical currents to image the conductivity distribution of the medium under investigation. It uses a two-dimensional array of electrodes placed on the ground, collecting conductivity data from stimulation of pair wise combinations of electrodes as shown in Figure (2-5). The data are then post-processed with an algorithm that gives an image of the conductivity profile of the subsurface volume. Because both metallic and nonmetallic mines create conductivity anomalies, the technology is appropriate for detecting all types of mines. Moreover, it is especially well suited for mine detection in wet environments, such as beaches or marshes, because of the enhanced conductivity of the moist substrate. The equipment is relatively simple and inexpensive. Its limitations in that the required physical contact with the ground may detonate a mine and it cannot be used in dry, non conductive surfaces.

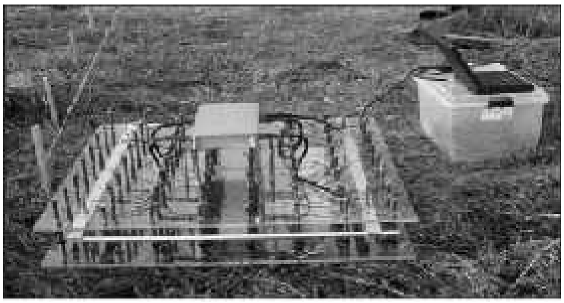

Figure (2-5) EIT Landmine Detector

2-3.3 X-Ray Backscatter

Traditional x-ray radiography produces an image of an object by passing photons through the object. X rays have a very small wavelength with respect to landmine sizes, so in principle they could produce high-quality images of mines. It operates by detecting the difference in the atomic number between the ground and the mine target **[6]**. The backscatter technique uses X-ray photons that bounce off the electrons of materials. Explosives and plastics rebound back more photons than soil does, and they scatter them more widely, which can create more accurate images of the mines. Rocks, wood, roots and other materials create very different images and cannot be confused with land mines. However, the applicability of this technology is limited due to the limited penetration of the x-rays into the ground**.**

2-3.4 Infrared/Hyper-spectral Systems

The use of thermal IR technique is based on the thermal radiation contrast of objects, with respect to their backgrounds. All objects at temperatures greater than absolute zero emit electromagnetic (EM) radiation at wavelengths from 3μm to 100μm is referred to as the thermal IR radiation. The magnitude of spectral radiations of an object depends on its temperature **[7]**. For landmine detection, landmines are thought of as a thermal barrier in the natural flow of the heat inside the soil, which produces a perturbation of the expected thermal pattern on the surface. The detection of these perturbations (anomalies) will put into evidence the presence of potential landmine targets.

2-3.5 Ground-Penetrating Radar (GPR)

GPR detects buried objects by emitting radio waves into the ground and then analyzing the return signals generated by reflections of the waves at the boundaries of materials with different indexes of refraction caused by differences in electrical properties. Generally, reflections occur at discontinuities in the dielectric constant, such as at the boundary between soil and a landmine or between soil and a large rock. A GPR system consists of one antenna or series of antennas that emit the waves and then pick up the return signal. A small computerized signal-processing system interprets the return signal to determine the object's shape and position.

So this thesis deals with study of GPR antenna, we will talk in more details about GPR technique in the next chapter.

2-4 Acoustic/Seismic Techniques

In this method, sensors sense differences in mechanical properties of the mine and soil. Sound waves above the ground can penetrate into the ground surface due to poro-elastic nature of the soil or granular nature of road construction materials. The sound energy coupled into the ground causes seismic motion of the ground surface and subsurface, called acoustic-to-seismic (A/S) coupling. Landmines buried in the subsurface will resonate and induce distinct changes in the seismic motion due to scatter and reflection of the sound energy coupled into the ground. Specialized sensors can detect these vibrations without contacting the ground. A variety of different kinds of sensors (laser Doppler vibrometers, radars, ultrasonic devices, microphones) have been tried **[8]**.

Acoustic/seismic systems have the potential for very low false alarm rates. In experiments to date, false alarms from naturally occurring clutter, such as rocks and scrap metal, have been extremely low (although such hollow clutter items as soda bottles and cans would cause false alarms because the resonance patterns of these objects are similar to those of mines). An additional strength, these sensors are unaffected by moisture and weather, although frozen ground may limit the sensor's capability. The greatest limitation of these systems is that they do not detect mines at depth because the resonant response attenuates significantly with depth. With current experimental systems, mines deeper than approximately one meter diameter are difficult to find **[4]**.

2-5 Explosive Vapor Detection Techniques (EVD)

Such type of techniques deals with detecting release explosive vapor or chemical derivatives in landmine surrounding. Different types of explosives are utilized as the main charge in antipersonnel and antitank landmines. However, the most commonly used explosive in landmines is TNT. About eighty percent of different types of landmines manufactured worldwide contain TNT or mixtures of explosives containing TNT **[9]**.When a mine is buried in the soil, it almost always will gradually release explosives or chemical derivatives to the surrounding soil through either leakage from cracks and seams or vapor transport through the mine casing (in the case of plastic mines) **[4]**.

Explosive Vapor Detection techniques **(**EVD) consist of both biological and chemical methods.

2-5.1 Biological Methods

These methods deals with use mammals (e.g. dogs and rats), insects (bees), or microorganisms (bacteria) to detect explosives.

• **Dogs and Rats:** This kind of mammals use sense of smell to detect the explosive vapor. Dogs have a strong sense of smell, so by offering dogs reward of food or play, they can be trained to signal when they smell explosive vapor. Then the handler follows the dog and investigate the area by probe.

Rats likely would have similar strong sense of smell, Rats have an advantages over dogs, it is too light (1-1.5 kg) to set off mines.

• **Bees**: Bees have an acute sense of smell. Entomologists have trained bees to detect a variety of explosives and have been researching ways to use trained bees in humanitarian demining. Trained bees detect explosives and they also potentially could search a relatively large area in a short time**,** it has been found through a series of repeated trials conducted in 2001 and 2002 bees behaved like a fine-tuned detector at vapor levels higher than 10 parts per trillion (pptr) from 2.4-dinitrotoulene (2.4-DNT) mixed in sand **[10]**. Further, bees can only work under limited environmental and weather conditions, they do not fly during heavy rain or wind, and when temperatures drop to near or below freezing.

• **Bacteria:** A bacterial mine detection process would involve spraying bacteria on the mine-affected area, possibly using an airborne system. The bacteria would be allowed to grow for several hours. Bacteria can be engineered to be highly specific to the explosive of concern hence reducing false alarms. It can also cover a large area in a short time. They found that such bacteria, when applied to soil, will glow if the soil is contaminated with solvents like toluene or xylene. TNT is closely related to these solvents chemically, so it was fairly simple to modify these bacteria to fluoresce in its presence **[10]**. The method has been tested mainly in lab environment with test over a simulated minefield where in both cases mines were located successfully, but real-world conditions may not be similar. In the field, this method could allow for searching hundreds of acres in a few hours, which is much faster than other techniques, and could be used for area reduction and on a variety of terrain types. While it needs more time to adequately test the technique in real minefield.

2-5.2 Chemical Methods

Chemical techniques use arrays of polymer-based sensors that detect explosive vapors and other volatile chemicals based on the amount of swelling in the polymers caused by exposure to the analytic of concern. These swelling differences, in turn, lead to easily detected changes in electrical resistance of the polymers.

• **Fluorescent Polymers Sensor**: This sensor consists of two glass slides, each covered by a thin film of the fluorescent polymer. When a sample of air containing explosives passes between the slides, some of the explosive binds to the polymer and in the process temporarily reduces the amount of fluorescent light that the slides emit. A small photo-multiplier device detects the reduced light emission, and electronics signal the operator that explosives are present.

Nomadics Inc. has developed a man-portable prototype of this system and has conducted limited field tests. The current system can detect explosive vapor concentrations as low as 10–15 g per milliliter, and additional development work is expected to lower this threshold.

However, both biological and chemical methods for detecting explosive vapors currently are limited by incomplete knowledge of how explosive vapors migrate in the shallow subsurface.

2-6 Mechanical Techniques

Mechanical techniques used for landmine detection are those which have a physical contact with mines, they are may be manual such as Prodder or motorized such as Clearing Machines.

2-6.1 Prodders and Probes

Prodding is one of the most adopted techniques used by deminers to identify the cause of a signal detected via other detection systems. A classical prodder generally is composed by a non magnetic needle (for situations where a magnetic device could activate mines) about 25 cm long, the deminer scans the soil at a shallow angle of typically 30°. Each time he detects an unusual object, he assesses the contour, which indicates whether the object is a mine. The probe operator learns through experience to feel or hear the difference between a mine casing and other buried objects.

2-6.2 Mine Clearing Machines

When there is not a lot of time for an army to clear a minefield, it will often employ the use of certain machines to roll through and clear a safe path. Military forces employ several kinds of mine-clearing machines to clear out or detonate mines as shown in Figure (2-6). Some machines are specifically designed for the task of mine clearance, while tanks can also be fitted with certain mine-clearing devices. There are several types of mine-clearing machines. New machines are remote controlled, which minimizes the risk to personnel. Mine-clearing machines use one of three techniques, including flailing chains to beat the ground, rollers to roll over and detonate mines, and rakes or blades to plow through the minefields, pushing the mines to the side. These methods are quick and efficient and there is less chance of people getting injured during demining **[11]**. However this leaves the area virtually destroyed. Plush land for farmers etc will be destroyed also machines can easily miss mines.

Figure (2-6) Mine Clearing Vehicle

2-7 Comparison Between Landmine Detection Techniques

Table (2-1) shows the comparison between landmine detection techniques presents in this chapter.

Table (2-1) Comparison Between Landmine Detection Techniques

Technique			Operating Principle	Strengths	Limitations
Electromagnetic	Electromagnetic Induction		Change in the magnetic field	Cheap and easy to use	Low metal content mines, metal clutter
	Electrical impedance tomography		Uses electrical currents to image the conductivity distribution of the medium	Relatively simple and inexpensive	Physical contact with the ground may detonate a mine and it cannot be used in dry, non conductive surfaces
	X-Ray Backscatter		Images buried objects with x rays	Produce high-quality images of mines	Limited penetration and radiation effects
	Infrared/Hyper-spectral Systems		Based on the thermal radiation contrast of objects	Operates from safe standoff distances and scans wide areas quickly	
	Ground-Penetrating Radar (GPR)		Reflections of the waves at the boundaries of materials with different indexes of refraction	Detect metal or non-metallic mines	Roots, water pockets, other natural clutter; extremely moist environments
Acoustic/Seismic			Differences in mechanical properties of the mine and soil	Unaffected by moisture and weather	Deep mines; vegetation cover; frozen ground
Explosive Vapor Detection	Biological Methods	Dogs	Detecting release explosive vapor or chemical derivatives in landmine surrounding	Unaffected by metal clutter	Expensive training
		Rats		Unaffected by metal clutter, light weight don't trigger mines	
		Bees		Search a relatively large area in a short time	Effected by weather conditions
		Bacteria		Cover a large area in a short time	Not tested in real minefield
	Chemical Methods	fluorescent polymers		Detect low explosive vapor concentrations	Very dry environments
Mechanical methods	Prodders and Probes		Instill a stick into ground to difference between a mine casing and other buried objects.		Physical contact with mine, i.e. trigger mines
	Mine Clearing Machines		Heavy force to donate mines and remove them side.	Quick and efficient and safe	Destroyed and Plush land, easily miss mines

Chapter 3

Electromagnetic Wave Propagation in Materials

3-1 Introduction

The knowledge of the electric and magnetic properties of materials over a broadband frequency range is an important requirement to know how electromagnetic wave propagate in that materials.

The electric and magnetic properties of materials usually depended on several factors such as: water content, temperature, linearity, isotropy, homogeneity and so on.

Many researchers have shown experimentally that for most materials which constitute the shallow sub-surface of the earth, the attenuation of electromagnetic radiation rises with frequency and that at a given frequency, wet materials exhibit a higher loss than dry ones **[12]**.

The most important microwave characteristics of soils are; electrical permittivity (ε), magnetic permeability (μ) and electrical conductivity (**σ**). Magnetic permeability (μ) becomes significant only in a ferromagnetic materials **[3]**.

3-2 Electromagnetic parameters of ground.

Electromagnetic parameters of ground that affect the propagation of radio waves include electrical permittivity (ε), magnetic permeability (μ) and electrical conductivity (**σ**). Variations in EM properties of soils are caused by physical factors such as lithology, porosity, water content, and water salinity. These parameters will be described briefly in the following subsections.

3-2.1 Dielectric permittivity (ε)

Dielectric permittivity is defined as the ability of a medium to store electromagnetic energy in the form of induced charge polarization and then permit to the passage of EM energy when an external field is imposed on the material **[13]**.

Dielectric permittivity also referred to dielectric constant is commonly represented by relative dielectric constant (ε_r), which is the ratio of the dielectric permittivity of material to the permittivity of free space (ε_o) as in equation (3-1)

$$£_r = \frac{£}{£_0} \quad \text{[dimensionless]} \qquad (3\text{-}1)$$

Where $£_0 = 8.854 \cdot 10^{-12}$ *F/m*

Change in dielectric constant of material mainly depended upon water content of that material.

3-2.2 Magnetic permeability (μ)

Magnetic permeability can be defined as the ability of material to store (or get magnetized) and dissipate when electromagnetic field is imposed on it. Also it can be defined as the ease of magnetic field propagation in material. Magnetic permeability is complex quantity with the real part describing storage component and the imaginary part describing dissipation component as stated in equation (3-2) **[13]**.

$$«_r = \frac{«}{«_0} \quad \text{[dimensionless]} \qquad (3\text{-}2)$$

Where $\mu_\circ = 4\pi * 10^{-7}$ H/m

Non-magnetic materials (i.e., most rocks and soils) have very little effect on the propagation of EM waves, the value of $\mu \simeq \mu_\circ$, hence their relative permeability is approximately equal to one. However media that contain magnetic minerals, iron-oxide cement, and iron-rich soils have a relative magnetic permeability high enough to attenuate electromagnetic wave during transmission **[13]**.

3-2.3 Electrical conductivity (σ)

Electrical conductivity is the ability of a material to conduct (transmit) an electrical current and it is commonly expressed in units of milli-Siemens per meter (mS/m)**[14]**. Electrical Conductivity also defined as the ability of material to transport electric charge **[13]**. Conductivity values of different soil materials are shown in Figure (3-1) below.

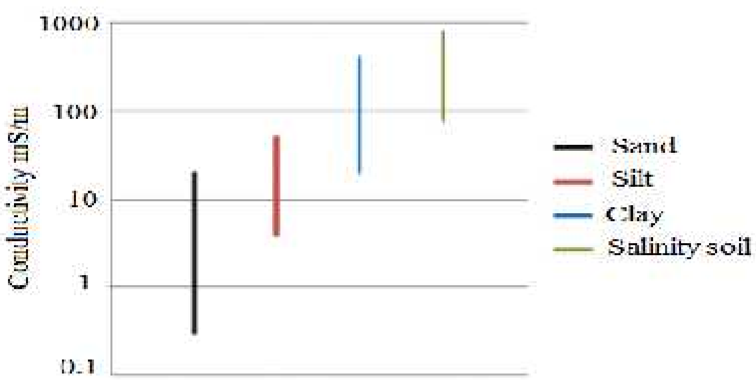

Figure (3-1) Conductivity Values of Different Soil Materials.

3-3 Electromagnetic Wave Propagation in Dielectric Materials

Electromagnetic waves propagating through natural media experience losses to both the electric *(E)* and magnetic *(H)* fields. This causes attenuation of the original electromagnetic wave. For most materials of interest in ground-penetrating radar, the magnetic response is weak and need not be considered as a complex quantity, unlike the permittivity and conductivity, so absorption of electromagnetic radiation is caused by both conduction and dielectric effects. The electromagnetic wave propagation in dielectric materials is primarily governed by the relative permittivity of a material, which depends primarily upon its water content. At microwave frequencies, including the range over which GPR systems operate, water has a relative permittivity of about 80, while the solid constituents of most soils and man-made materials have, when dry, a relative permittivity ***εr*** in the range 2 to 9 **[12]**. The absolute permittivity also varies with frequency, but is generally constant for most materials over the range of frequencies utilized for GPR . Table (3-1) shows the relative permittivity and electrical conductivity of various materials **[12]**.

Table (3-1) Relative Permittivity and Electrical Conductivity of Various Materials

Material	Relative Permittivity	Conductivity S/m
Air	1	0
Asphalt: dry	2-4	$10^{-2}:10^{-1}$
Asphalt: wet	6-12	$10^{-3}:10^{-1}$
Clay: dry	2-6	$10^{-1}:10^{0}$
Clay: wet	15-40	$10^{-1}:10^{0}$
Coal: dry	3-5	$10^{-3}:10^{-2}$
Coal: wet	8	$10^{-3}:10^{-1}$
Concrete: dry	4-10	$10^{-3}:10^{-2}$
Concrete: wet	10-20	$10^{-2}:10^{-1}$
Freshwater	81	$10^{-6}:10^{-2}$
Freshwater ice	4	$10^{-4}:10^{-3}$
Granite: dry	5	$10^{-8}:10^{-6}$
Granite: wet	7	$10^{-3}:10^{-2}$
Limestone: dry	7	$10^{-8}:10^{-6}$
Limestone: wet	8	$10^{-2}:10^{-1}$
Permafrost	4-8	$10^{-5}:10^{-2}$
Rock salt: dry	4-7	$10^{-4}:10^{-2}$
Sand: dry	2-6	$10^{-7}:10^{-3}$
Sand: wet	10-30	$10^{-3}:10^{-2}$
Sandstone: dry	2-5	$10^{-6}:10^{-5}$
Sandstone: wet	5-10	$10^{-4}:10^{-2}$
Sea water	81	10^{2}
Sea-water ice	4-8	$10^{-2}:10^{-1}$
Shale: dry	4-9	$10^{-3}:10^{-2}$
Shale: saturated	9-16	$10^{-3}:10^{-1}$
Snow firm	6-12	$10^{-6}:10^{-5}$
Soil clay: dry	4-10	$10^{-2}:10^{-1}$
Soil clay: wet	10-30	$10^{-3}:10^{0}$
Soil loamy dry	4-10	$10^{-4}:10^{-3}$
Soil loamy wet	10-30	$10^{-2}:10^{-1}$
Soil sandy dry	4-10	$10^{-4}:10^{-2}$
Soil sandy wet	10-30	$10^{-2}:10^{-1}$

Maxwell's equations are the foundation for the consideration of the propagation of electromagnetic waves in dielectric materials.

Electromagnetic wave propagation can be represented by a one-dimensional wave equation as in equation (3-3).

Propagation is taken along the z-axis, with perpendicular electric field *(E)* and perpendicular magnetic field *(H)* as shown in Figure (3-2).

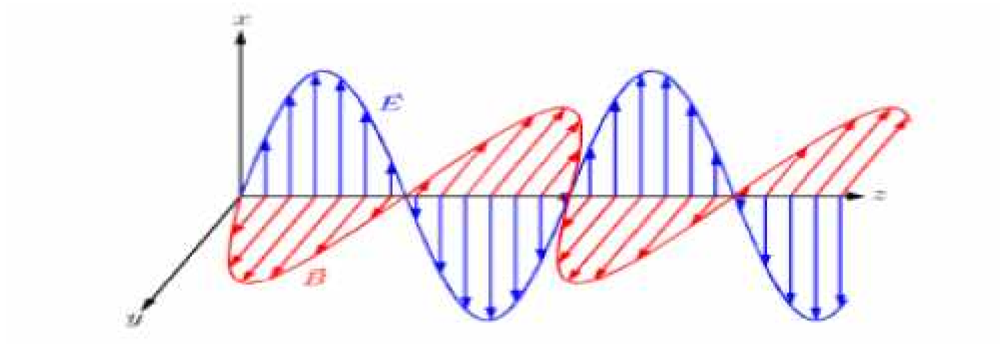

Figure (3-2) Propagation of Electromagnetic Waves in Free Space

$$\frac{\partial^2 E}{\partial Z^2} = \text{«£} \frac{\partial^2 E}{\partial t^2} \qquad (3\text{-}3)$$

In practice, most generators produce voltages and currents which vary sinusoidally. Corresponding electric and magnetic fields also vary sinusoidally with time. This implies that the $\partial E/\partial t \rightarrow -j\omega E$ and $\partial^2 E/\partial t^2 \rightarrow -\omega^2 E$.

The wave equation becomes:

$$\nabla^2 E = -\mu\varepsilon\omega^2 E + j\mu\sigma\omega E \equiv \gamma^2 E \qquad (3\text{-}4)$$

Where

$$\gamma^2 = -\mu\varepsilon\omega^2 + j\mu\sigma\omega \qquad (3\text{-}5)$$

$$\text{¥} = \mu\sqrt{\text{«£}\left(1 + j\frac{\pm}{\mu\text{£}}\right)} \qquad (3\text{-}6)$$

Where γ is a propagation constant.

In general the parameters of interest for ground penetrating radar applications are the attenuation, velocity of wave propagation and intrinsic impedance of the medium.

Propagation constant can be written as:

$$\gamma = \alpha + j\,\beta \qquad (3\text{-}7)$$

By squaring equation (3-5) and equating it to equation (3-5), it can be seen that α and β have the same sign.

Then the attenuation factor α can be written as

$$α = ω \sqrt{\left[\frac{«£}{2}\sqrt{1+\left(\frac{±^{2}}{µ^{2}£^{2}}\right)}-1\right]} \tag{3-8}$$

and a phase constant β

$$β = ω \sqrt{\left[\frac{«£}{2}\sqrt{1+\left(\frac{±^{2}}{µ^{2}£^{2}}\right)}+1\right]} \tag{3-9}$$

The intrinsic impedance of the medium ¦ can be defined as the ratio between electric field E to the magnetic field H where ¦ =E/H.

$$¦ = \sqrt{\frac{-jµ«}{± - jµ£}} = \sqrt{\frac{«/£}{1-j\frac{±}{µ£}}} \tag{3-10}$$

So the propagation of an electromagnetic field in a conducting dielectric material can be described by E(*z*,*t*) at a distance, *z*, and time, *t*, by:

$$E(z,t) = E_0 \cdot e^{-\sim z} \cdot e^{j(µt- \ z)} \tag{3-11}$$

From the above equations it can be noted that the value of the ratio σ/ωε is a good measure to decide whether a material is a dielectric or a metal.

For good conductors, it takes σ/ωε ≫ 1

$$\sim = \quad = \sqrt{\frac{µ±«}{2}} \tag{3-12}$$

and the velocity of the wave in the conductor is

$$¬ = \frac{µ}{\ } = \sqrt{\frac{2µ}{«±}} \tag{3-13}$$

The wave is greatly attenuated inside a conductor. Depth of penetration or ***skin depth*** δ is defined as the distance at which an electromagnetic wave would have attenuated to 1/e of its value on the surface. Skin depth provides an indication of the penetration depth of a ground-penetrating radar system.

$$\delta = \frac{1}{\alpha} = \sqrt{\frac{2}{\omega\mu\sigma}} \qquad (3\text{-}14)$$

For conductors like copper this distance is typically less than a fraction of a millimeter. However, this study deals with lossy dielectric media which exhibit polarization damping losses in addition to possible finite conductivity losses. So even though $\boldsymbol{\sigma}$ may be zero, it will simply use a complex permittivity ($\boldsymbol{\varepsilon' - j\varepsilon''}$) and include any conduction loss as part of the imaginary component of $\boldsymbol{\varepsilon''}$ as shown in Figure (3-3).

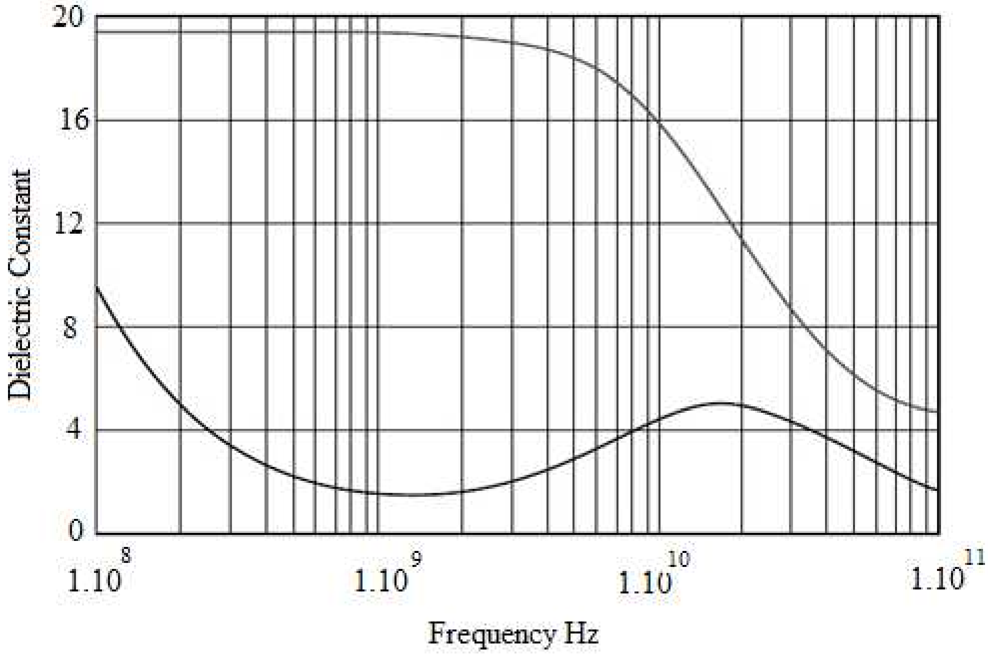

Figure (3-3) Dielectric Properties ε' (Upper) and ε'' (Lower) of Lossy Soil as a Function of Frequency.

So the previous relations become:

$$\gamma = \alpha + j\,\beta = \omega\sqrt{\mu\varepsilon'\left(1 - j\frac{\varepsilon''}{\varepsilon'}\right)} \qquad (3\text{-}15)$$

$$\alpha = \omega\sqrt{\left[\frac{\mu\varepsilon'}{2}\sqrt{1 + \left(\frac{\varepsilon''}{\varepsilon'}\right)^2} - 1\right]} \qquad (3\text{-}16)$$

$$\beta = \omega \sqrt{\left[\frac{\mu \varepsilon'}{2} \sqrt{1 + \left(\frac{\varepsilon''}{\varepsilon'} \right)^2} + 1 \right]} \qquad (3\text{-}17)$$

$$\eta = \sqrt{\frac{\mu}{\varepsilon' \left(1 - j \frac{\varepsilon''}{\varepsilon'} \right)}} \qquad (3\text{-}18)$$

The factor ($\frac{\varepsilon''}{\varepsilon'}$) is more commonly called material loss tangent and usually symbols by (tan δ). Loss tangent includes dielectric damping loss and conductivity loss of a material. The two types of loss are distinguishable to each other, it is frequency dependant.

For ***lossless material***, there is no loss and (tan δ = 0), the permittivity is real and is simply $\varepsilon = \varepsilon_0 \varepsilon_r$

3-4 Effect of Water Content of the Soil on the Propagation

As it has mentioned in the previous section, the wave propagation in dielectric materials is primarily governed by the relative permittivity of a material, which depends primarily upon its water content**.**

Water content of the soil can change dramatically within the course of hours, days, and years. This change in soil water content around the landmine can strongly effect landmine detection. Some researchers (Das et al., 2000; Borchers et al., 1999; Hendrickx et al., 1990 and Topp et al., 1980) studied the dependence of dielectric constant on the volumetric water content of different soil mixtures. In their study they choose a radar system with a 1-MHz to 1-GHz variable frequency range. A series of 18 different experiments were carried out to determine the influence of selected parameters on the relationship between water content and the apparent dielectric constant **[15]**. For these experiments the apparent dielectric constant was measured, which assumed that the electrical loss was insignificant and that the apparent dielectric constant was approximately equal to the real part of the dielectric constant. Since the effects of electrical loss existed in their estimate of the real part of the dielectric constant (ε'), they called the measured dielectric constant an apparent dielectric constant (ε_a) **[15]**. Thus for low-loss, nearly homogenous materials it is assumed that:

$$\varepsilon' \simeq \varepsilon_a \qquad (3\text{-}19)$$

From their experiments using many different soil types they were able to find the following empirical relationship between the apparent dielectric constant (ε_a) and volumetric soil water content (θ).

$$\varepsilon_a = 3.03 + 9.3\,\theta + 146.0\,\theta^2 - 76.7\,\theta^3 \qquad (3\text{-}20)$$

Figure (3-4) shows the relation between volumetric water content versus dielectric constant using equation (3-20).

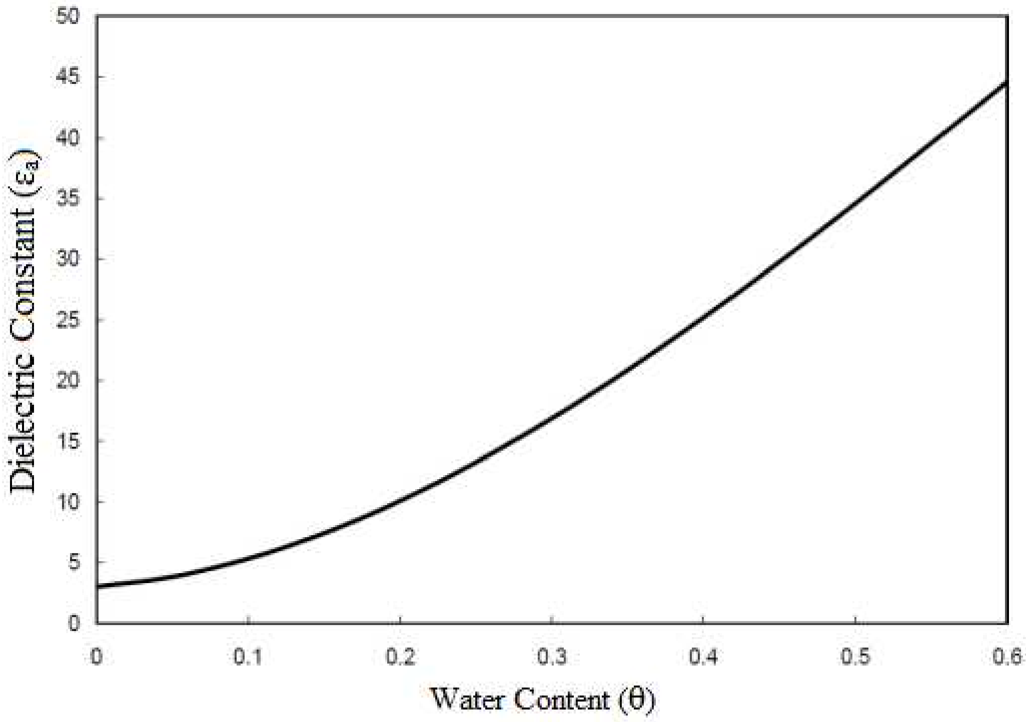

Figure (3-4) Volumetric Water Content versus Dielectric Constant Using Equation (3-20)

Chapter 4

Ground Penetrating Radar (GPR)

4-1 Introduction

The terms ground penetrating radar (GPR), ground-probing radar, sub-surface radar or surface-penetrating radar (SPR) refer to a range of electromagnetic techniques designed primarily for the location of objects or interfaces buried beneath the earth's surface or located within a non-visually structure **[12]**. GPR is a high-resolution electromagnetic technique used to evaluate the location and depth of buried objects and to investigate the presence and continuity of natural subsurface conditions and features, without drilling, probing, or digging. GPR is one of a number of technologies that has been mentioned in previous chapter as a means of improving the efficiency of landmine clearance operations. The technology of GPR has many different applications and the overall design is usually dependent on the target type and the material of the target and its surroundings. The range of applications for GPR methods is wide and the complexity of signal recovery techniques, hardware designs and operating practices is increasing as the technology progress.

Performance of GPR is depending upon the surface and subsurface conditions and its specifications include requirements for or information about reflections, depth of investigation, resolution. The ability at which GPR can detect objects is depending on the wavelength of the input signal, so the quality of the image improves as the wavelength decreases and the frequency increases. But, at high frequencies, the GPR penetration of the incident wave into the soil can be poor. At Low frequency the penetration is more but with less resolution. However, the design of GPR system must make a trade-off between quality of the image and required penetration depth. The optimal design for maximizing image quality while ensuring sufficient penetration depth changes with environmental conditions, soil type, mine size, and mine position. Recently, alternative GPR are being explored to optimize the trade of between penetration depth and image quality under a wide range of conditions. Moreover the signal-processing is considered to be the most critical part in the design of a GPR system. In fact it is the process that filters out clutter signals and selects objects to be declared as mines.

4-2 GPR Applications

GPR has many applications in a number of fields**;** it has been used in the following fields:

- **Geological fields:**

-Detection natural cavities and fissures

-Subsidence mapping.

-Mapping of superficial deposits

-Soil stratigraphy mapping

-Geological structure mapping

-Mapping of faults, dykes, coal seams

-Lake and riverbed sediment mapping

-Mineral exploration and resource evaluation

• **Engineering and construction**

- Detection of landmines and unexploded ordinance

-Road pavement analysis

-Void detection

-Location of reinforcement (rebars) in concrete

-Location of public utilities (pipes, cables, etc.)

-Testing integrity of building materials

-Concrete testing

-Tunnel investigations

-Soil conductivity mapping

• **Environmental Investigations**

-Contaminated soil investigation

-Hazardous material delineation

• **Other applications:**

-Mapping of Groundwater Resources

-planetary exploration

-forensic investigations

-medical imaging

-Snow thickness Measurement

-Remote sensing from aircraft and satellites

-Archaeological research

-Cemetery Mapping

4-3 GPR working principle

GPR operates by transmitting electromagnetic wave that is radiated from a transmitting antenna down into the ground as shown in Figure (4-1). When the transmitted signal enters the ground, it contacts objects or subsurface strata with different electrical conductivities (**σ**) and dielectric constants ($\boldsymbol{\varepsilon_r}$). Part of the ground penetrating radar waves reflect from the object or interface, while the rest of the waves pass through to the next interface.

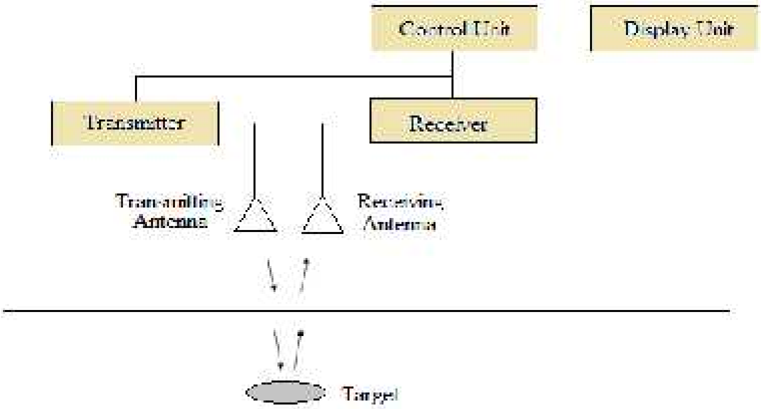

Figure (4-1) Working Principle of GPR

The reflected signals return to the antenna, pass through the antenna, and are received by the digital control unit. The control unit registers the reflections against two-way travel time in nanoseconds and then amplifies the signals. The time between transmission and reception, referred to as the two-way travelling time (TWTT) and commonly measured in nanoseconds, is a function of reflector depth and the EM velocity of propagation. GPR provides a continuous profile of the subsurface, displaying horizontal survey distance against vertical TWTT. Vertical TWTT is converted to depth with knowledge of the propagation velocity, expressed as in equation 4-1)

$$d = \frac{v*t}{2} \tag{4-1}$$

Where d is depth, v is velocity, and t is TWTT.

4-4 GPR Types

GPR system design can be classified into two groups**,** *Impulse GPR and Continuous Wave GPR,* which are described in the following points:

• **Impulse GPR:** In impulse radars, a time domain pulse is transmitted (narrow pulse, less than a few nano-seconds), and reflected wave is received as a function of time. The waveforms generated in the display unit show the amplitude of energy reflected from the underground objects versus time. Most of the ground-penetrating radar systems which are built around the impulse technique send a pulse to an antenna, which in turn produces an electromagnetic wave. The center frequency of the electromagnetic wave is determined by the properties of the antenna, and the corresponding bandwidth is determined by the pulse width. It is clear to see that the antenna plays a significant role in the GPR systems.

• **Continuous Wave GPR:** Continuous wave radars acquire and continuously transmit data on the reflected energy as a function of frequency. This technique is divided into two sub-techniques, swept frequency or stepped frequency over a fixed bandwidth.

• **Swept frequency CW GPR:** The concept involves transmitting a frequency sweep over a fixed bandwidth from start frequency to a stop frequency. The reflected energy is received as a function of frequency and indicated the amplitude of energy scattered from the subsurface object. Then the received signal is mixed or heterodyned with a portion of transmitted signal filtered and sampled during the sweep, then the sampled waveform from the entire sweep transformed into time domain to obtain a synthesized pulse.

• **Stepped Frequency CW GPR:** The stepped frequency continuous radar is similar to Swept frequency CW system except the transmitting frequency stepped in linear increments Δf over a fixed bandwidth. At each frequency the amplitude and phase of the received signal is sampled and recorded. The received signal is transformed into the time domain using Inverse Discrete Fourier Transform (IDFT) to obtain a synthesized pulse. In the case of the stepped frequency continuous wave radar system, direct coupling of the transmitted and received signals lead to dynamic range problems. The main advantage of the SFCW ground penetrating radar over the pulsed system is that the former has a higher average radiated power for transmission.

4-5 GPR System

There are five main components that make up a working GPR system as shown in Figure (4-2).

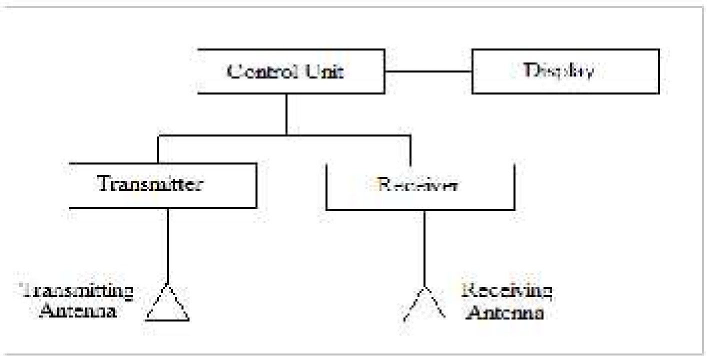

Figure (4-2) GPR System Components

These components can be stated as follows:

-Transmitter: The transmitter consists of a signal generator and a power amplifier, the signal generator produces a pulse, amplified by the power amplifier and then applied to transmitting antenna.

-Receiver: The receiver of GPR consists of a sampling unit, a filtering and amplifying unit**.**

-Control unit: Control unit controls in both transmitter and receiver, it triggers the transmitter to emit a short pulse wave into space via the transmitting antenna. At the same time, the control unit also sends a command to the sampling unit to set the unit ready for the coming reflected signals

-Display unit: Display unit is used to visualize the target in an user-friendly manner, which may be lab top computer, printer, etc...

-Antenna: The most critical component in a GPR system is the antenna which is the main subject of this thesis. In most GPR systems they have used *bistatic* scheme (two antennas one for transmitting and other for receiving) or *monostatic* scheme (one antenna for transmitting and receiving) which couples the signal (energy) from the transmitter into the ground and receives the reflected signal from the ground (or target), so in the next section we will try to give brief idea for antenna parameters.

4-6 Antenna parameters

In this section we will try to review some of antenna parameters which describe the antenna performance, especially that are related to GPR environment such as input impedance, beam width, reflection coefficient, transient response, VSWR and front to back ratio.

Radiation pattern: An antenna radiation pattern or antenna pattern is defined as a mathematical function or a graphical representation of the radiation properties of the antenna as a function of space coordinates.

The radiation pattern is measured in the far-field region, where the spatial (angular) distribution of the radiated power does not depend on the distance. The *field patterns* (magnitude of the electric or magnetic field) $|\mathbf{E}(\theta,\varphi)|$, $|\mathbf{H}(\theta,\varphi)|$ or *power patterns* (square of the magnitude of the electric or magnetic $|\mathbf{E}(\theta,\varphi)|^2 / \eta$ or $\sim \eta\ |\mathbf{H}(\theta, \varphi)|^2$ are shown in Figures (4-3) and (4-4).

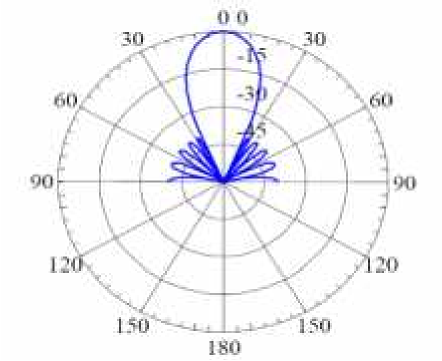

Figure (4-3) Polar Representation of Pattern

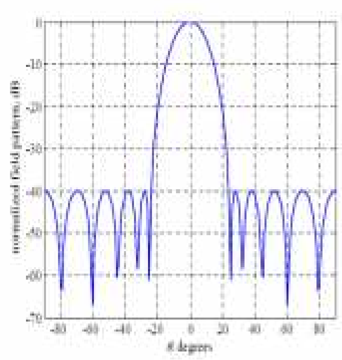

Figure (4-4) Rectangular Representation of Pattern

Half Power BeamWidth HPBW: Antenna beamwidth is measured in degrees between the half power points (3 dB) of the main lobe of the antenna, as shown in Figure (4-5). The beam width of the antenna is also used to describe the resolution capabilities of the antenna to distinguish between two adjacent radiating sources or radar targets.

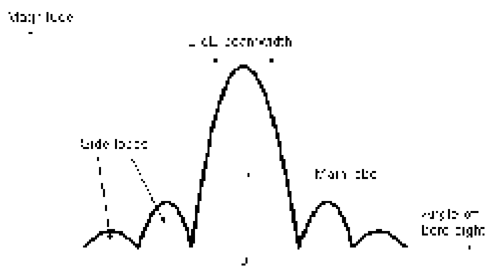

Figure (4-5) Antenna Half Power BeamWidth

Directivity: The directivity of an antenna can be defined as the ratio of the radiation intensity in a given direction from the antenna to the radiation intensity averaged over all directions, where the average radiation intensity is total power radiated by the antenna divided by 4π. another more simply definition is the directivity of a non-isotropic source is equal to the ratio of its radiation intensity in a given direction to that of an isotropic source.

Antenna Gain: *Gain* of an antenna (in a given direction) is defined as "the ratio of the intensity, in a given direction, to the radiation intensity that would be obtained if the power accepted by the antenna were radiated isotropically. The radiation intensity corresponding to the isotropically radiated power is equal to the power accepted (input) by the antenna divided by 4π." In most cases, the reference antenna is a lossless isotropic source **[16]**.

Input Impedance Z_{in}: The Input impedance presented by an antenna at its terminals defined as the ratio of the voltage to current at a pair of terminals or the ratio of the appropriate components of the electric to magnetic fields at a point. Figure (4-6) shows the antenna equivalent circuit antenna represented by its impedance *Za* connected to the voltage source with its impedance *Zs* by using transmission line of impedance Z_o.

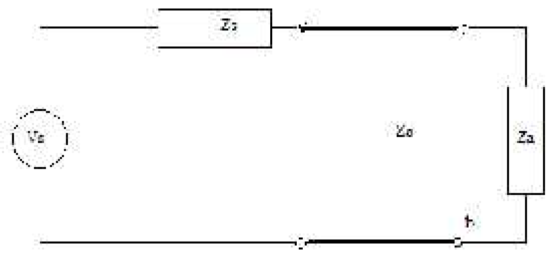

Figure (4-6) Antenna Equivalent Circuit

If an impedance of a transmission line (Z_0) (which connect the antenna to the source) and the antenna impedance (Za) are not identical then there will be a mismatch to the antenna terminals and some of the incident signal will be reflected back to the source.

Reflection Coefficient and VSWR: The reflection coefficient (Γ) is defined as ratio of the reflected voltage (V_0^-) to the transmitted voltage (V_0^+), and Γ is given by the equation (4-2).

$$\Gamma = \frac{V_0^-}{V_0^+} = \frac{Z_a - Z_0}{Z_a + Z_0} \qquad (4\text{-}2)$$

The other parameter frequently used to characterize impedance matching is Voltage Standing Wave Ratio (VSWR). The VSWR is defined as the ratio of the peak voltage maximum to peak voltage minimum in the standing wave pattern at an impedance discontinuity which is given by the equation (4-3).

$$VSWR = \frac{1+|\Gamma|}{1-|\Gamma|} \qquad (4\text{-}3)$$

For the perfect matching VSWR=1, there is no reflection and return loss. In the reality systems it is very hard to achieve a perfect match over a wide frequency match so it is accepted that VSWR < 2 is still good matching system.

Antenna Bandwidth BW: The bandwidth of an antenna is defined as "the range of frequencies within which the performance of the antenna, with respect to some characteristic, conforms to a specified standard." **[16]**

Ultra wide-bandwidth is defined when the system has a an operating bandwidth greater than 20% measured at the (-10dB point of S_{11} or < 2 for VSWR), where narrow bandwidth is less than 1% at the (-10dB point of S_{11} or < 2 for VSWR). A system is also considered UWB if the operating bandwidth is greater than 500MHz **[17].**

Antenna Field Regions: The space surrounding an antenna is usually subdivided into three regions: (1) reactive near-field, (2) radiating near-field (Fresnel) and (3) far-field (Fraunhofer) regions as shown in Figure (4-7). These regions are so designated to identify the field structure in each **[16].**

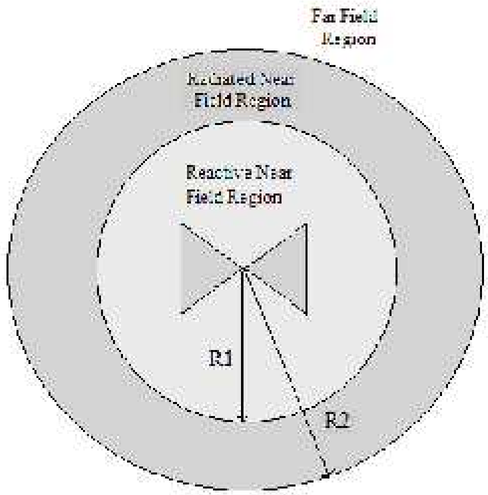

Figure (4-7) Antenna Field Regions

Where $R_1 = 0.62\sqrt{\frac{D^3}{\lambda}}$, $R_2 = \frac{2D^2}{\lambda}$

Reactive near-field region: It's the region immediate vicinity of the antenna, in this region the reactive fields are predominately.

***Radiating near-field region**:* It's the region of the field of an antenna between the reactive near-field region and the far-field region wherein radiation fields predominate. If the antenna has a maximum overall dimension which is very small compared to the wavelength, this field region may not exist **[16]**.

***Far-field region**:* It is commonly taken to exist at distances greater than $2D^2/\lambda$ from the antenna, λ being the wavelength.

4-7 GPR Antenna Requirements

Usually GPR antenna works very close to the ground, which is lossy and dispersive, therefore the electrical properties of the ground will have a strong influence on the antenna's parameters, which acts as low pass filter. The total detection times for GPR systems are usually less than 100 ns. For shallow targets it can be even a few nanoseconds **[18]**. Therefore, the transmitting signal should have a very short time duration and the antenna must be able to transmit the signal with little distortion and less ringing in order to avoid masking of the target reflection. This requires an antenna with broadband properties and very short impulse response. Antenna for GPR system must have the following characteristics:

1. Good coupling of EM energy into the ground, i.e. good impedance matching at the antenna/ground interface.
2. Low and short time ringing (ringing occurs due to reflection from the antenna ends).
3. High power-handling capability so that the signal can achieve adequate depth of penetration to reach a target with sufficient amplitude to generate a receivable return signal.
4. Adequate bandwidth to benefit from both larger penetration depth of low-frequency signals, as well as the high range resolution of higher-frequency signals.
5. Have impedance that is well matched across the entire bandwidth in the actual operating setup where the antenna is near to the ground.
6. Provide high directivity, concentrating EM energy into a narrow solid angle into the ground.
7. Provide weak coupling between transmit and receive antennas in a bistatic mode.
8. Be compact enough to occupy a reasonably small volume.

4-8 Bowtie Antenna for GPR System

Bow-tie antenna is an approximated transfiguration between biconical antenna and dipole antenna as shown in Figure (4-8). Biconical antennas have broadband characteristics but it is not simple to construction, dipole antennas have narrowband characteristics but it is simple to build, so bowtie antennas is a trade-off between the two antennas, quite broadband characteristics and simple to construction.

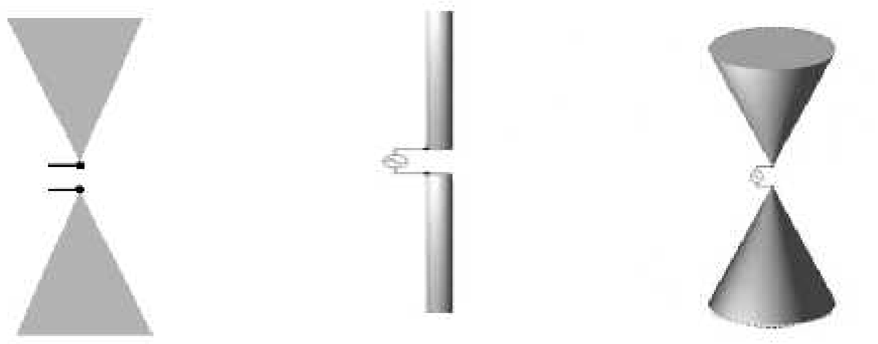

(a) (b) (c)

Figure (4-8) Bow-tie Antenna (a) an Approximated Transfiguration Between, Dipole Antenna (b) and Biconical Antenna (c)

4-9 Antenna Ringing

Impulse GPR requires an ultra-wideband antenna system capable of transmitting properly short transient pulses. In certain GPR applications for detection of ground subsurface and shallow-buried objects such as landmines, the antenna should exhibit a very low level of late-time ringing in order to prevent masking of radar targets. When an ideal GPR antenna is excited, it radiates only during the duration of the excitation pulse. But in reality, the antenna continues to radiate even after the excitation pulse has died down. This is due to the internal reflections of the charges that occur at the ends of the bowtie wings and the excitation points. The charges move back and forth in the bowtie wings, gradually decaying and radiating at discrete time intervals into the external media. This is known as antenna ringing **[19]**. Figure (4-9) shows antenna ringing in far field time response of radiating pulse.

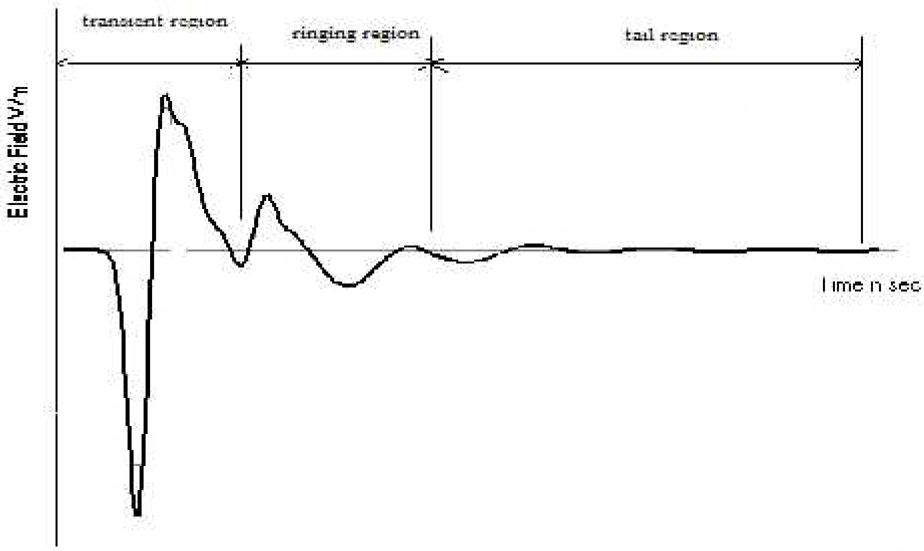

Figure (4-9) Antenna Ringing in Far Field Time Response of Radiating Pulse

Antenna ringing is undesirable as it corrupts the transmitted pulse waveform and reduces range resolution. A conventional method to reduce it (i.e. increasing the antenna's bandwidth) is the implementation of a resistive loading **[20]**. unfortunately, this method decrease the antenna efficiency, also wide-bandwidth antenna lead to high frequency, i.e. low depth of penetration, so the trade-off between antenna ringing and antenna efficiency and also between range resolution and depth of penetration should be made. Consequently, in the next chapter an optimization of bowtie antenna by using finite difference time domain method (Remcom XFDTD version 6.3 Three-dimensional full wave electromagnetic analysis package software) will be done to achieve the above trade-offs.

Chapter 5

FDTD Simulation for GPR Antenna

5.1 Introduction

The Finite Difference Time Domain (FDTD) method, introduced in 1966 by K.S. Yee. In the FDTD approach, both space and time are divided into discrete segments. Space is segmented into box-shaped “cells”, which are small compared to the wavelength. The electric fields are located on the edges of the box and the magnetic fields are positioned on the faces as shown in Figure (5-1).

Time is quantized into small steps where each step represents the time required for the field to travel from one cell to the next **[21]**. Given the offset in space of the magnetic fields from the electric fields, the values of the field with respect to time are also offset. The electric and magnetic fields are updated using a leapfrog scheme where first the electric fields, then the magnetic are computed at each step in time.

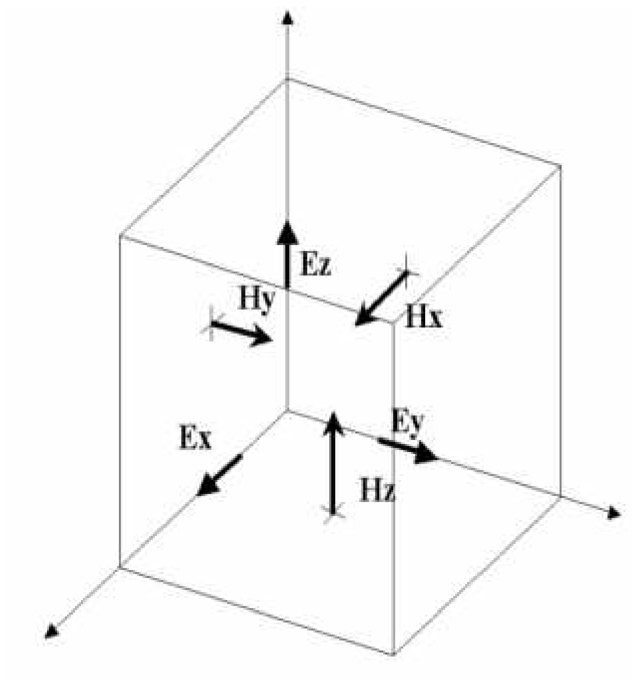

Figure (5-1) Yee Cell with Labeled Field Components.

When many FDTD cells are combined together to form a three-dimensional volume, the result is an FDTD grid or mesh. Each FDTD cell will overlap edges and faces with its neighbors, so by convention each cell will have three electric fields that begin at a common node associated with it. The electric fields at the other nine edges of the FDTD cell will belong to other, adjacent cells. Each cell will also have three magnetic fields originating on the faces of the cell adjacent to the common node of the electric fields as shown in Figure5-1.

5-2 FDTD Cell Size

The first step in the geometry design process is to define the size of the FDTD cell (Δ). By the FDTD method, the cell size (in x, y, and z directions) should be much less than the smallest wavelength of interest. The general rule is "10 cells per wavelength", that is, each cell side should be 1/10*l* or smaller at the smallest wavelength or highest frequency of interest, the antenna wavelength λ_U is given by:

$$\lambda_U = \frac{c}{f_U} \qquad (5\text{-}1)$$

Where *c* is speed of light ($3*10^8$ m/sec in free space)

f_U central frequency of antenna in Hz

5-3 FDTD Simulation of Bowtie Antenna

The X-Windows FDTD Graphical User Interface is a commercially available product marketed by REMCOM, Inc. The program, which uses the FDTD method for electromagnetic calculations, is a useful tool for modeling and simulating various electromagnetic problems such as antenna radiation scattering/penetration, microwave circuit calculations, and biological calculations.

The starting point of an FDTD calculation is often determining the spatial increment, or cell size, of the structure being simulated. we used a cell size of 0.5 cm in all directions (x, y and z).

The bowtie antenna used in simulations has dimensions as shown in Figure (5-2), and the thickness of sheet is 0.5 cm which made of perfect electrical conductor (PEC) material.

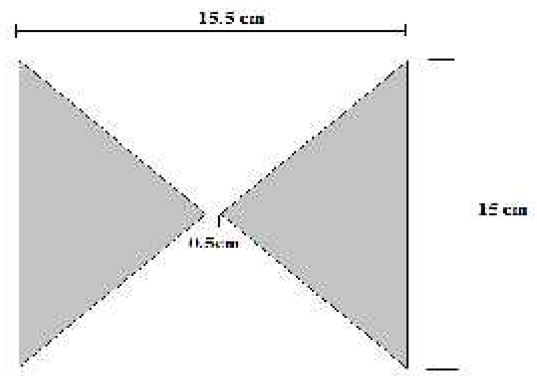

Figure (5-2) Dimensions of Bowtie Antenna

There are several factors to be considered when determining cell size.

(1)***Wavelength***: The primary constraint on cell size is wavelength. The FDTD cell can be no larger than 1/10 of the smallest wavelength used to excite the model **[22]**. Hence the maximum cell size may be determined from:

$$l_{m} = \frac{c}{1\ *f} \qquad (5\text{-}2)$$

Where l_{m} is the maximum cell dimension

c is the speed of light, $3x10*^{8}$ m/s in free space

f is the frequency of excitation (Hz)

(2) ***Geometry features***: The FDTD cell can be no larger than the smallest feature of your geometry so that the object can be represented accurately. For example, if the geometry contains two wires and the distance between them is smaller than the maximum cell size, a smaller cell size is needed.

(3) ***Accuracy***: Smaller cell sizes result in greater accuracy in the simulation.

5-3.1 Bowtie Antenna Dimension and Cell Size

The frequency band expected of our bowtie antenna is 700 - 1200 MHz with central frequency of 950 MHz, so the maximum allowable cell size using equation (5-2) is:

$$l_{m} = \frac{c}{1\ *f} = \frac{3*1\ ^{8}}{1\ *9\ \ *1\ ^{6}} = 0.031\ m \qquad l_{m} = 3.1\ c$$

Thus, the wavelength of central frequency is:

$$\lambda_{o} = \frac{c}{f_{o}} = \frac{3*1\ ^{8}}{9\ \ *1\ ^{6}} \cong 0.31\ m$$

Bowtie antenna length is $l = \frac{\lambda}{2} = \frac{0.3}{2} = 0.155\ m$

In this simulation a cell size is chosen to be 0.5 cm (i.e. $\Delta = 0.5$ cm) which is satisfying the factors of determining the cell size (i.e. smaller than 1/10 of the smallest wavelength used).

5-3.2 Antenna Feeding

The antenna is excited by Gaussian pulse of width 0.3 n sec, as shown in Figure (5-3), with amplitude of 100 v and the source impedance of 50 ohm .

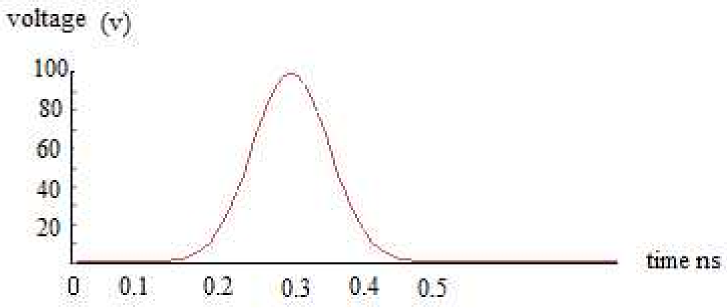

Figure (5-3) Input Signal (Gaussian Pulse)

5-3.3 Bowtie Antenna Field Regions

Bowtie antenna field regions, in the case of near field and far field boundaries, are determine by:

$R_1 = 0.62\sqrt{\frac{D^3}{\lambda}}$, $R_2 = \frac{2D^2}{\lambda}$

Where D = 0.155 m and $\lambda = 0.31\ m$,

Then $R_1 = 0.068$ m $R_2 = 0.155$ m

5-3.4 Depth of Penetration

The depth of penetration is mainly depended upon the ground conductivity, and the operating frequency. The following relation is used to calculate the skin depth:

$$\delta = \sqrt{\frac{1}{\pi \mu_o f_o \sigma}} \qquad (5\text{-}3)$$

where f_o (Hz) is the operating frequency, μ_o is the permeability of free space (= 4 π *10^{-7} H/m), and σ (S/m) is the ground conductivity.

Therefore, at 950 MHz operating frequency, for dry clay (conductivity (σ)= 0.01S/m), the skin depth would be 0.16 meters and for dry sand (conductivity (σ) = 0.0001S/m) would be 1.6 meters.

5-3.5 Simulation of Bowtie Antenna in Free Space

Once we determine the simulation parameters such as cell size, central frequency, input pulse waveform and near zone boundary, we start first simulation of bowtie antenna suspended in free space as shown in Figure (5-4).

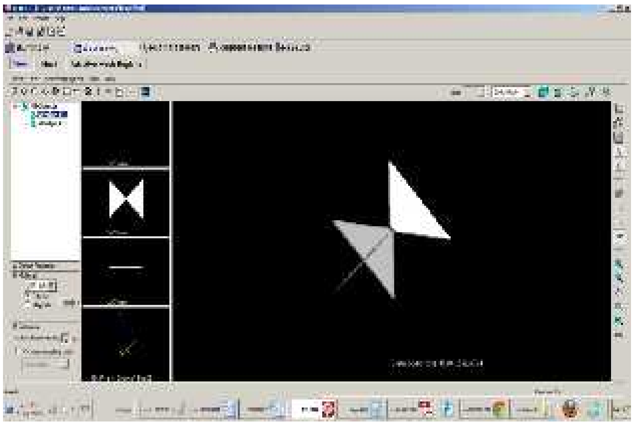

Figure (5-4) Simulation of Bowtie Antenna in Free Space by xfdtd UIG

At the beginning we use an excitation source with resistance of 50 ohm and observe the frequency response of antenna (VSWR and Input impedance) to know how our antenna works.

Figure (5-5) shows the VSWR vs. frequency, we note that the antenna has narrow bandwidth of range of about 120 MHz (480-600 MHz) as a result of a mismatching between antenna impedance and source impedance, and from Figure (5-6) that the antenna input impedance is not quite stable over frequency band.

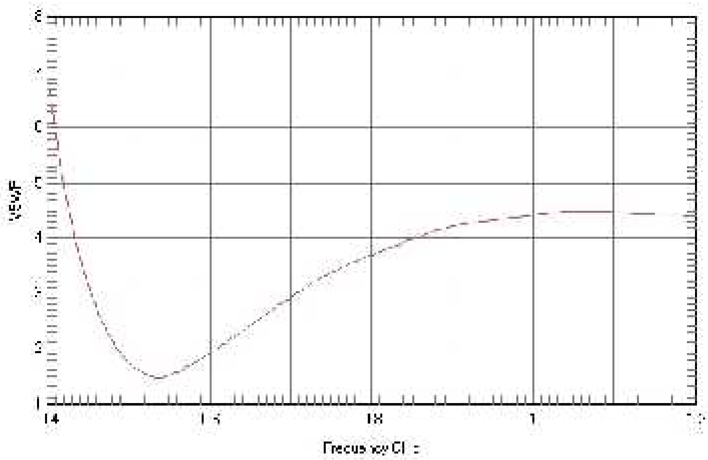

Figure (5-5) VSWR of Bowtie Antenna in Free Space

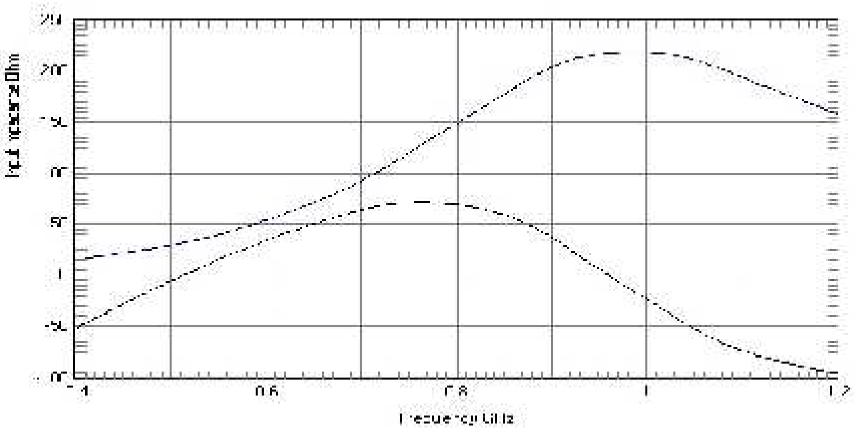

Figure (5-6) Input Impedance (*Real Part Above and Imaginary Part Below*) of Bowtie Antenna in Free Space**.**

Accordingly to matching antenna of impedance 220 ohm **[23]** to feeding source of impedance 50 ohm, a matching circuit should be used as shown in Figure (5-7.a).

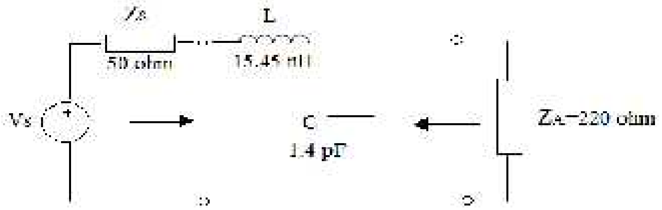

Figure (5-7.a) Equivalent Circuit of Antenna in Free Space with Matching Circuit

Values of L and C found by using LC impedance matching network designer software **[24]**, which its window is shown in Figure (5-7.b).

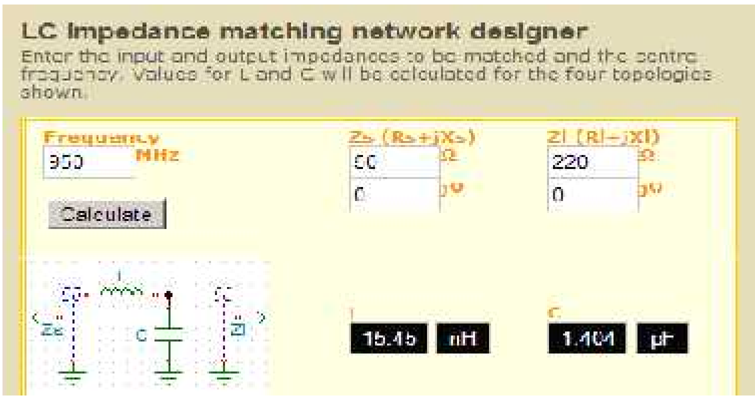

Figure (5-7.b) LC Impedance Matching Network Designer Software Window

Figure (5-8) shows the VSWR of antenna in free space with matching circuit, it's clearly that the antenna is suitable for operation over a frequency range (710-1280 MHz) i.e.

the antenna bandwidth (BW) is 570 MHz . and the input impedance is reasonable stable over a wide frequency range as shown in Figure (5-9).

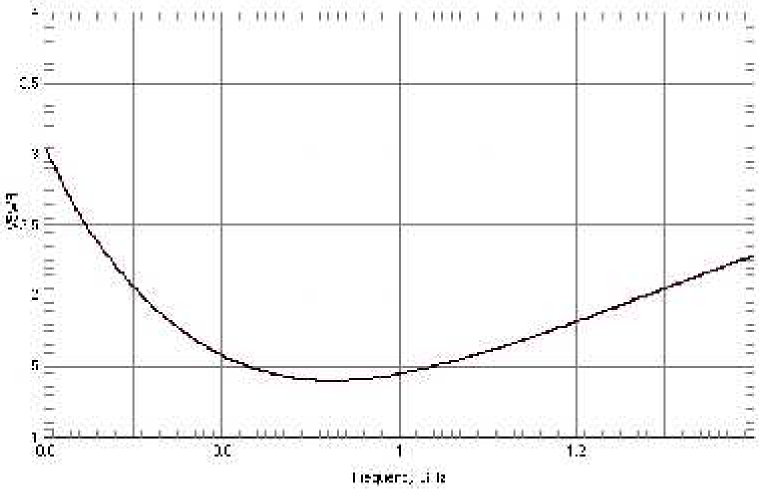

Figure (5-8) VSWR of Antenna in Free Space with Matching Circuit

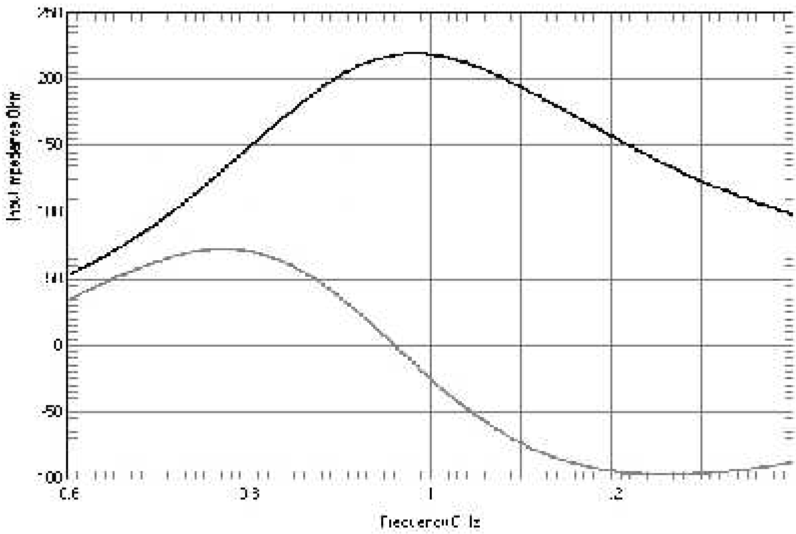

Figure (5-9) Input Impedance (*Real Part Above and Imaginary Part Below*) of Bowtie Antenna in Free Space with Matching Circuit.

5-3.6 Antenna Loading

As we have mentioned in chapter three, a conventional method to reduce late-time ringing (i.e. increasing the antenna's bandwidth) is the implementation of a resistive loading. The third simulation has been done by loading the antenna with resistors, Figure (5-10.a) shows the Electric far field versus time of bowtie antenna in free space without resistive load and Figure (5-10.b) shows the Electric far field versus time of bowtie antenna in free space with resistive load, we note a slight reduction in pulse ringing due to a resistive load.

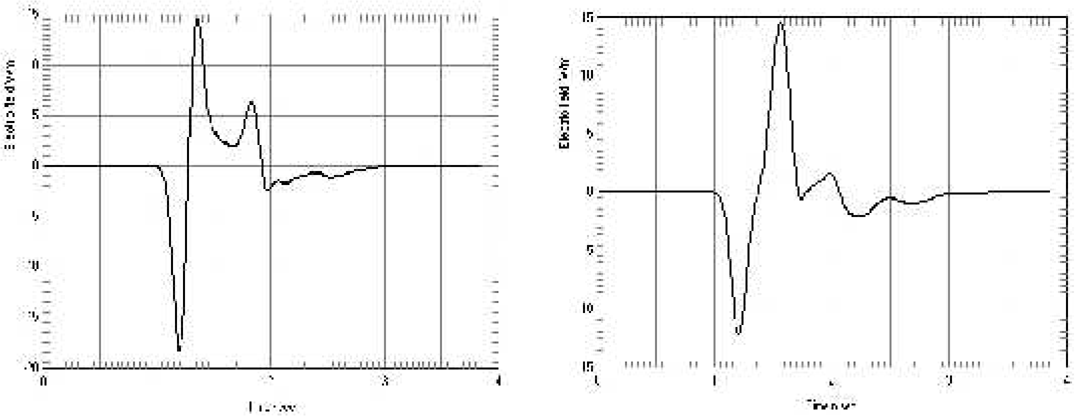

(a) (b)

Figure (5-10) Electric Far Field vs. Time of Bowtie Antenna in Free Space without (a) and with Resistive Load (b)

From Figure (5-11b) below it can be observed that a slight decrease in resistively loaded antenna gain compared with antenna without resistive load as shown in Figure (5-11a).

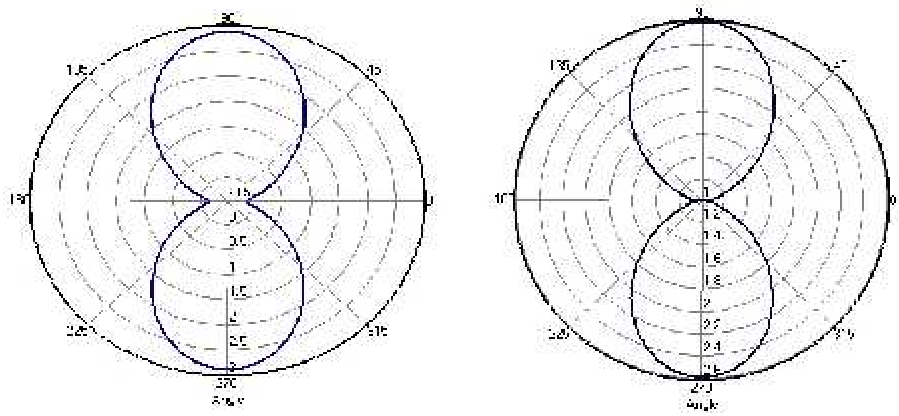

(a) (b)

Figure (5-11) Radiation Pattern of Bowtie Antenna in Free Space without (a) and with Resistive Load (b).

Also it can be observed from Figure (5-12) that the frequency response of a bowtie antenna in free space with resistive load has a slight decrease in bandwidth.

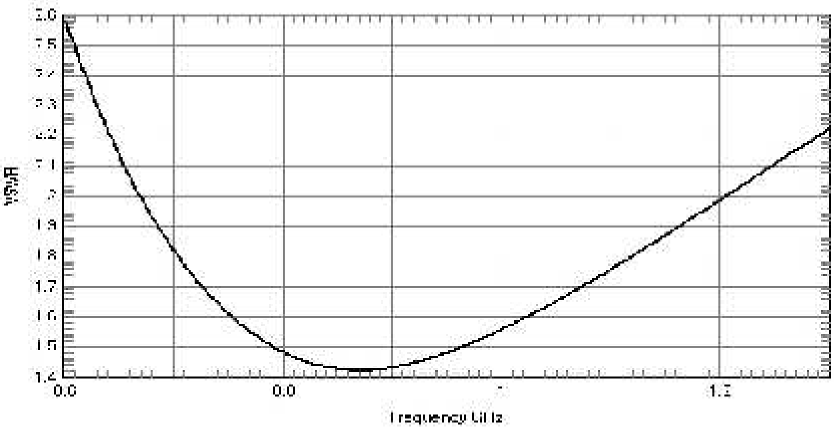

Figure (5-12) VSWR vs. Frequency of Antenna in Free Space with Resistive Load

5-3.7 Antenna Shielding

Most certainly for GPR system we need to concentrate most of the energy into the ground, this can be done by placing a copper shield over the antenna **[25]**, also it decreases the effect of any unwanted surrounding signals (above ground interference) and eliminate direct coupling between transmitting antenna and receiving antennas in case of bistatic GPR . Figure (5-13) shows bowtie antenna with copper shield.

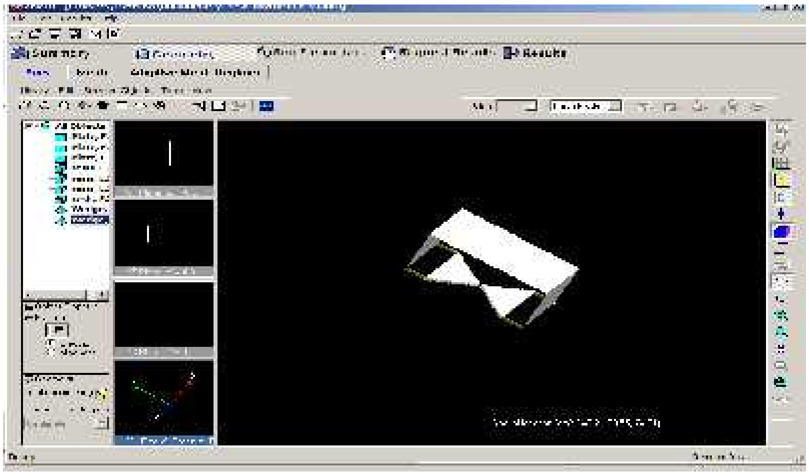

Figure (5-13) Bowtie Antenna with End Resistors and Copper Shield in xfdtd Window

In shielded bowtie antenna simulation we have used three heights of shield 5cm, 10cm and 15cm and observe the frequency response and radiation pattern of antenna.

From Figure (5-14) below its very clear that the bowtie antenna with 10cm shield height has better frequency response than others. Table (5-1) shows a antenna shield height and it's corresponding bandwidth .

Table (5-1) Antenna Shield Height and It's Corresponding Bandwidth.

Shield Height	Antenna Bandwidth
5 cm	180 MHz
10 cm	870 MHz
15 cm	670 MHz

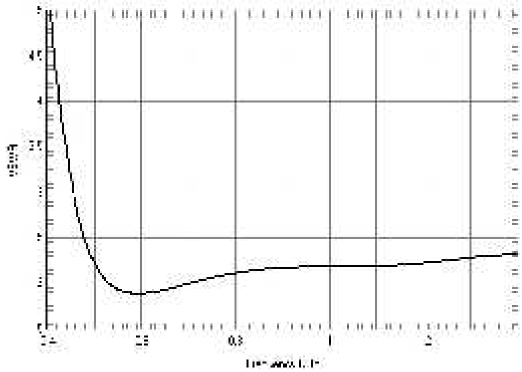

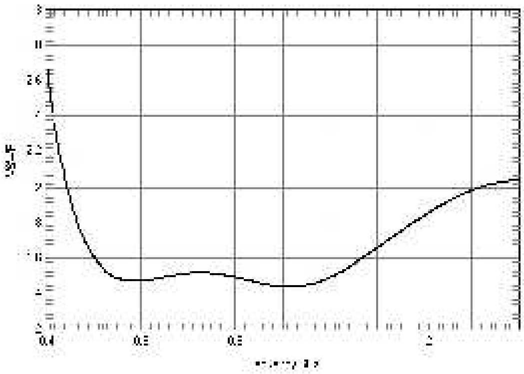

(a) (b)

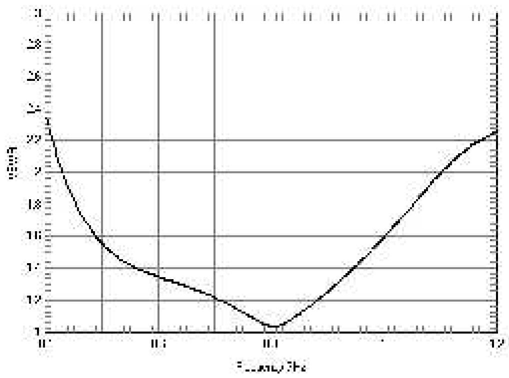

(c)

Figure (5-14) VSWR vs. Frequency of Bowtie Antenna with Resistive Load and Shield (a) 5 cm (b) 10 cm and (c) 15 cm Shield Height.

From the Figure (5-15) below, the antenna with shield height of 5cm has more desirable radiation pattern than others.

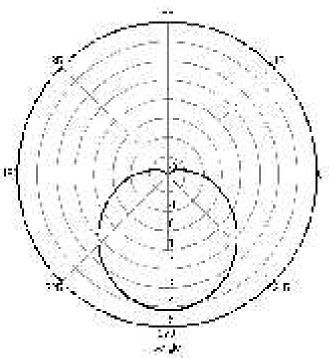

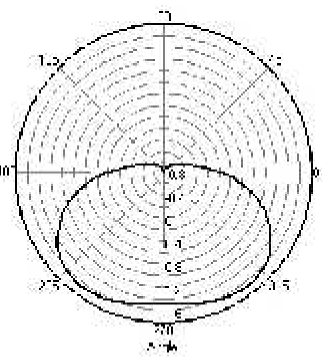

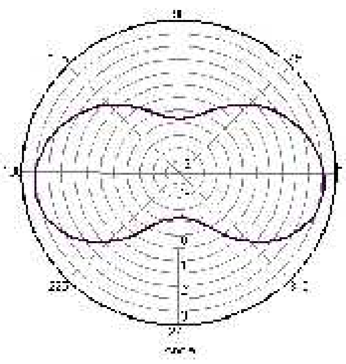

(a) (b) (c)

Figure (5-15) Radiation Pattern of Bowtie Antenna with Resistive Load and Shield (a) 5 cm (b) 10 cm and (c) 15 cm Shield Height.

From the Figure (5-16), it has been noted that the antenna shielding increases the ringing, antenna with shield height of 10 cm and shield height of 15 cm has a slightly less ringing than antenna with shield height of 5 cm.

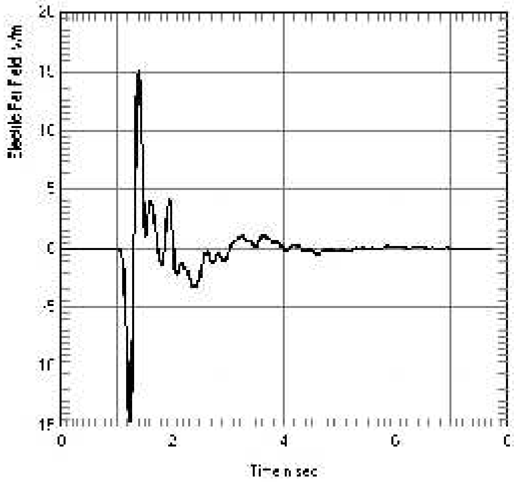

(a)

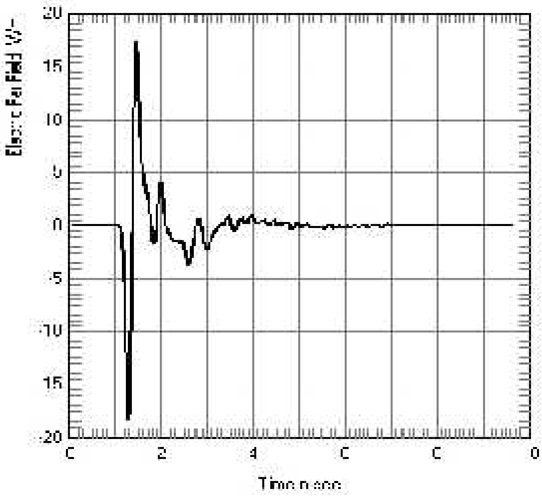

(b)

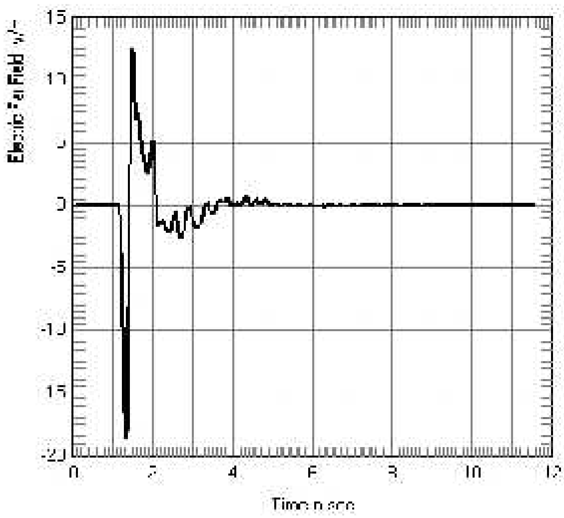

(c)

Figure (5-16) Electric Far Field vs. Time of Bowtie Antenna with Resistive Load and Shield (a) 5 cm (b) 10 cm and (c) 15 cm Shield Height

5-3.8 Antenna Shield Padding

To obtain more improvements for bowtie antenna characteristics over a wide frequency band, the inner walls of copper shield are padded by layers of gradually conductivity profile to act as electromagnetic absorbers that help absorb unwanted radiation in the upper half space. **[19][23]**.

A seven layer padding have been used with the conductivity profile of: $\sigma = 10^{n-4}$ where $n = 0,1,2,3,4,5,6$ is the layer number and $n = 0/$ is the number of layer just touching the air region inside the copper shield, each layer has a thickness of 0.5 cm (total padding thickness 3.5 cm). The geometry of bowtie antenna with padded copper shield simulation is shown in Figures (5-17) and (5-18).

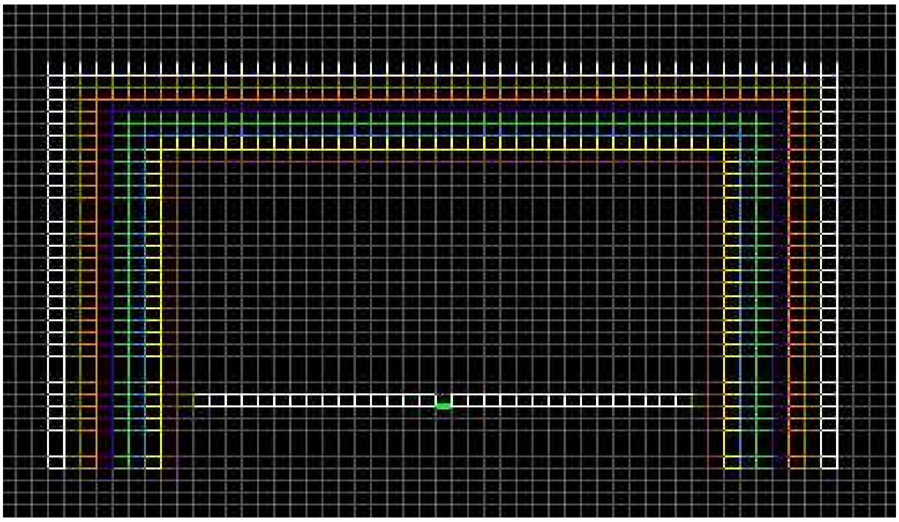

Figure (5-17) xfdtd Geometry of Bowtie Antenna with Padded Copper Shield

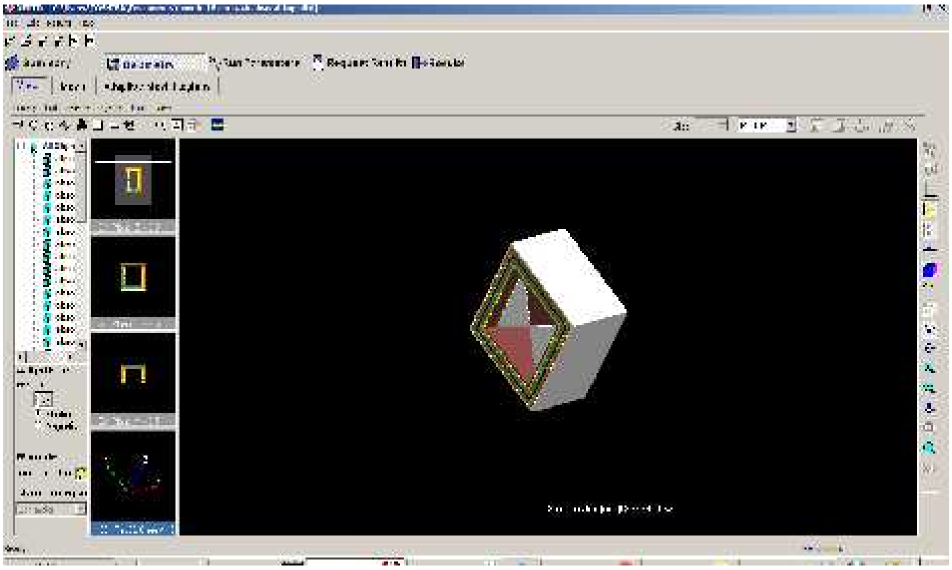

Figure (5-18) 3D - xfdtd Geometry of Bowtie Antenna with Padded Copper Shield

From Figures (5-19) and (5-20), bowtie antenna with padded copper shield has quite good characteristics, it's clear that the antenna bandwidth has improved (520 – 2170 MHz) about 1.65 GHz which is one important requirements for GPR antenna.

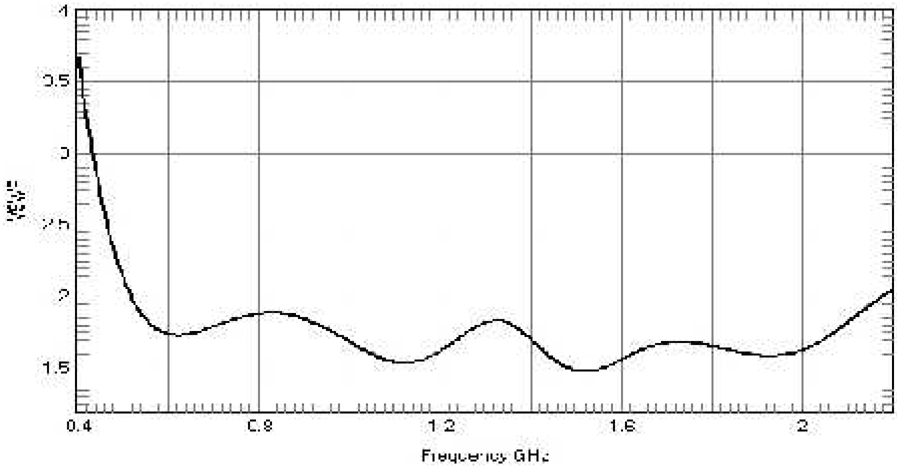

Figure (5-19) VSWR vs. Frequency of Bowtie Antenna with Padded Copper Shield

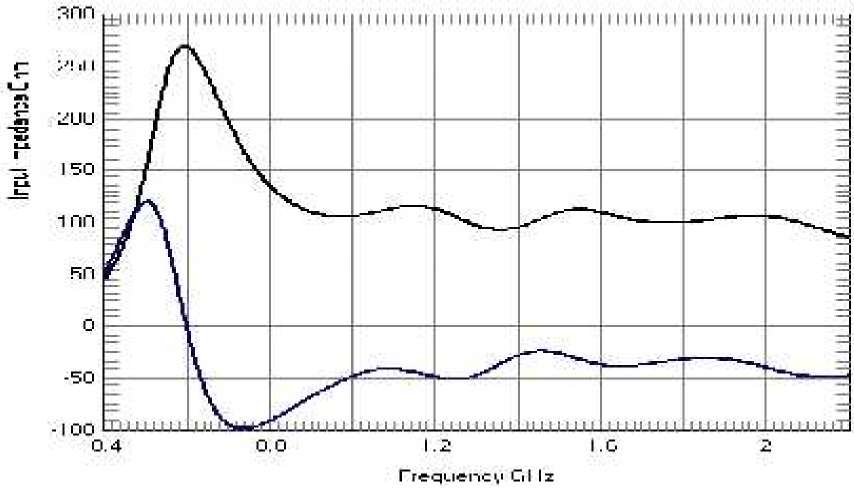

Figure (5-20) Input Impedance vs. Frequency of Bowtie Antenna with Padded Copper Shield

Bowtie antenna with padded copper shield has slightly low ringing than the antenna with copper shield only as shown in Figure (5-21).

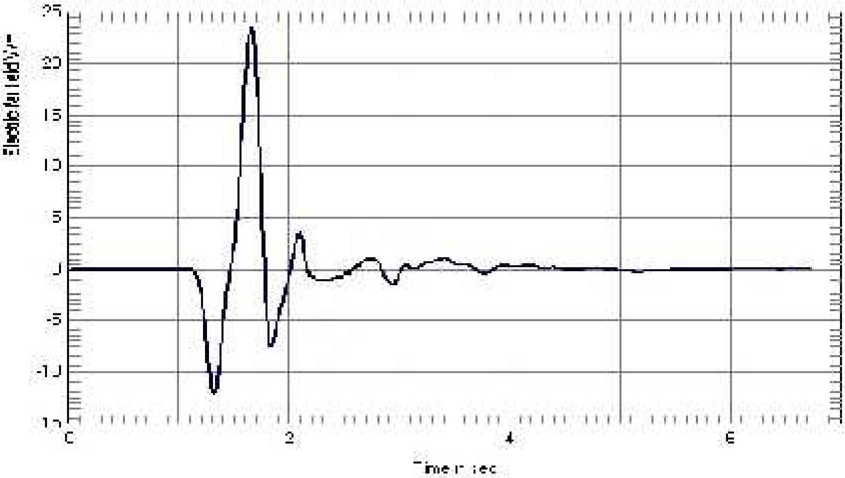

Figure (5-21) Voltage vs. Time at Feeding Point of Bowtie Antenna with Padded Copper Shield

Also from Figure (5-22) it has been noticed that the antenna with shield padding (electromagnetic absorber) has more desirable radiation pattern than without it i.e. the padding has a good effect on radiation pattern.

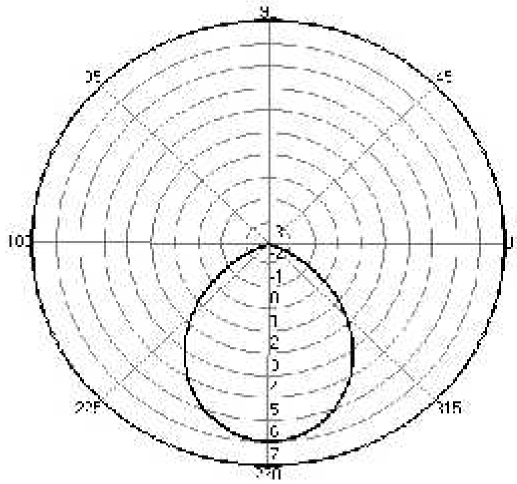

Figure (5-22) Radiation Pattern of Bowtie Antenna with Padded Copper Shield

5-4 Effect of Ground on Bowtie Antenna

After a pervious optimization of bowtie antenna we will examine the antenna with padded copper shield over two models of soils:

-Low losses soil (dry sand) ($\sigma = 10^{-5}$, $\varepsilon_r = 2.3$)

-Lossy soil (clay) ($\sigma = 10^{-1}$, $\varepsilon_r = 6$)

5-4.1 Bowtie Antenna over Low loss Soil (dry sand $\sigma = 10^{-5}$, $\varepsilon_r = 2.3$)

In this simulation bowtie antenna is placed at different heights over a low loss ground, just touch ground and 5 cm above ground surface as shown in Figure (5-23).

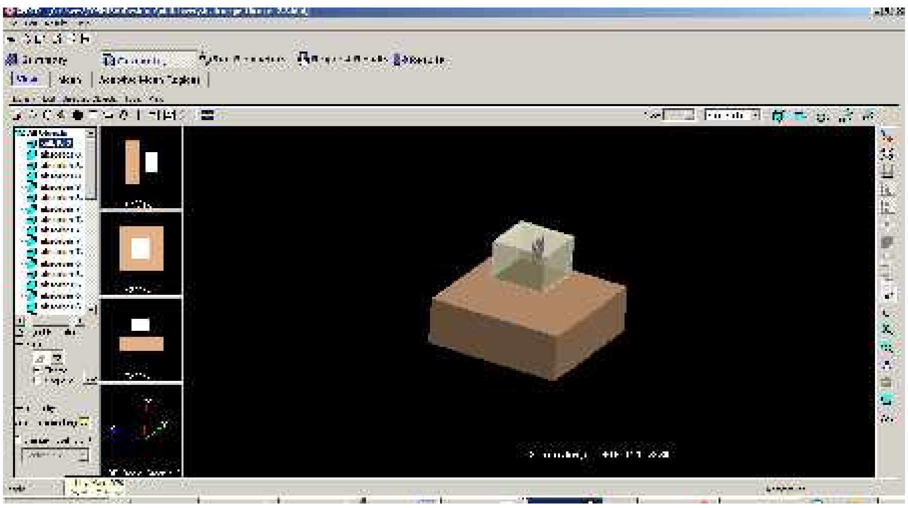

Figure (5-23) 3D-xfdtd Geometry of Bowtie Antenna with Padded Copper Shield Over Low Losses Soil

Figure(5-24.a) shows the effect of low-loss ground on bowtie antenna, frequency response of antenna is changed when antenna placed directly (touching ground) on ground surface, this change is undesirable i.e. reduces the antenna bandwidth), but when antenna placed at height of 5 cm above ground surface as shown in Figure (5-24.b), the frequency response of antenna becomes better.

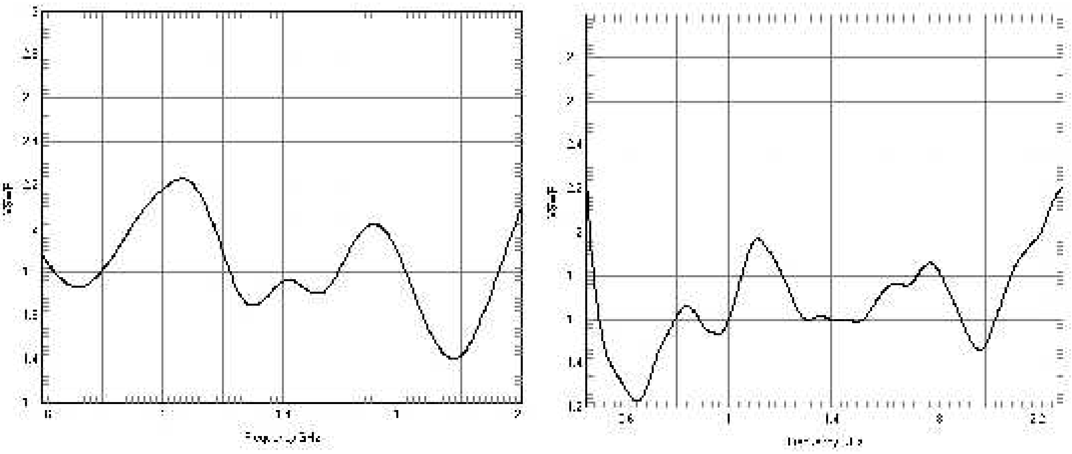

(a) (b)

Figure (5-24) VSWR vs. Frequency of Bowtie Antenna with Padded Copper Shield Over Low-loss Ground (a) Touch Ground (b) 5 cm Above Ground.

Also radiation pattern of 5 cm height shield is more desirable than that when antenna touch ground surface as shown in Figure (5-25).

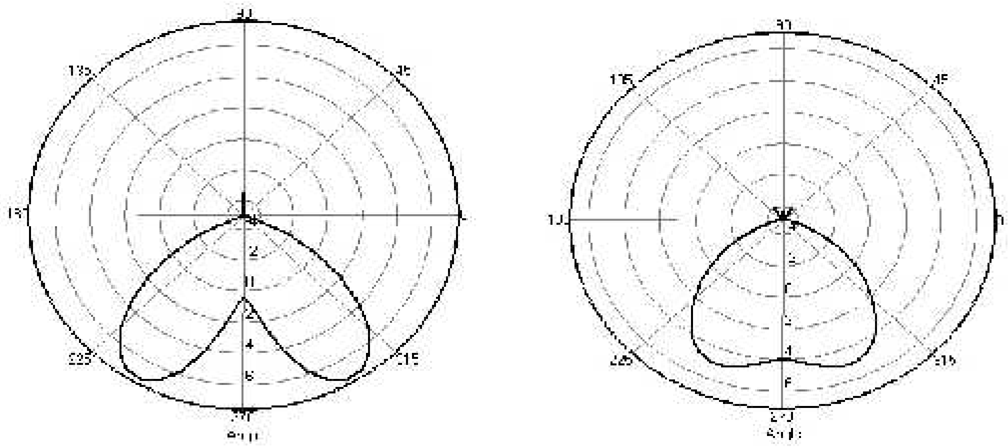

(a) (b)

Figure (5-25) Radiation Pattern of Bowtie Antenna with Padded Copper Shield Over Low losses Ground (a) Touch ground (b) 5 cm Above Ground.

5-4.2 Bowtie Antenna Over Lossy Soil (Clay $\sigma = 10^{-1}$, $\varepsilon_r = 6$)

As in the previous simulation, bowtie antenna is placed at different heights over a lossy ground ($\sigma = 10^{-1}$, $\varepsilon_r = 6$), just touch ground and 5 cm above ground surface.

From Figure (5-26.a), it's clear that the lossy ground (clay) has a bad effect on bowtie antenna frequency response when antenna placed directly (touching ground) on ground surface, but when antenna placed at height of 5 cm above ground surface, the antenna performance becomes better as shown in Figure (5-26.b).

Also radiation pattern at 5 cm height is more desirable than that when antenna touch ground surface as shown in Figure (5-27). From two simulation above its clear that the clay has worse effect on bow tie antenna characteristics than that of dry sand.

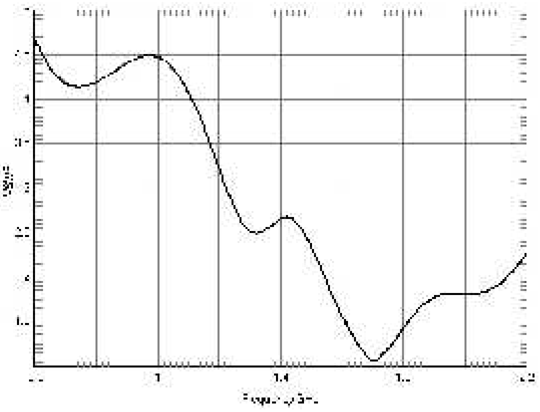

(a) (b)

Figure (5-26) VSWR vs. Frequency of Bowtie Antenna with Padded Copper Shield Over (Clay) Lossy Ground (a) Touch Ground (b) 5 cm Above Ground..

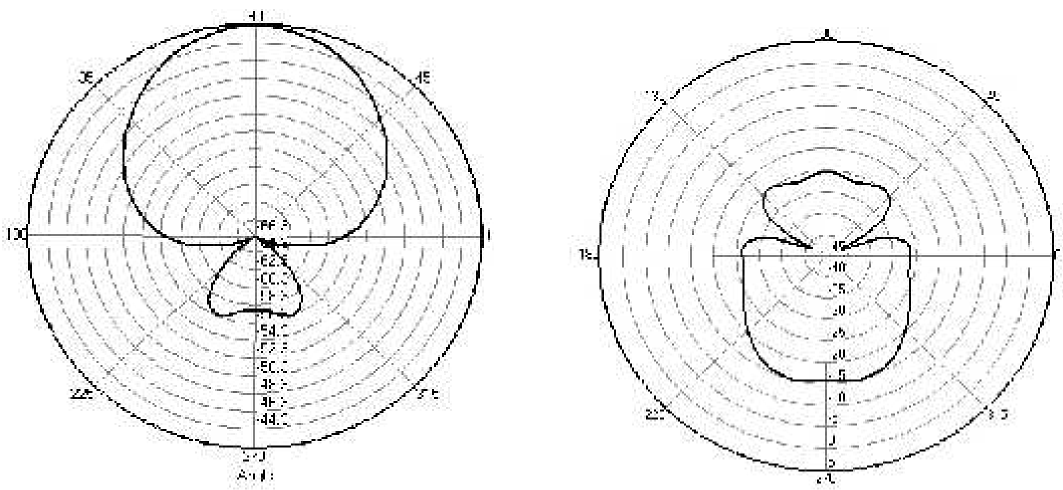

(a) (b)

Figure (5-27) Radiation Pattern of Bowtie Antenna with Padded Copper Shield Over (Clay) Lossy Ground (a) Touch Ground (b) 5 cm Above Ground.

5-5 Using of Two Bowtie Antennas as GPR System and Its Capability to Detect Targets

Two bowtie antennas are used to work as GPR system one antenna for transmitting and another for receiving, as shown in Figure (5-28) below.

The capability of the GPR system to detect buried targets can be measured from the change of the coupling (transmission coefficient $|S_2|$) between transmitting antenna and receiving antenna **[25][23]**.

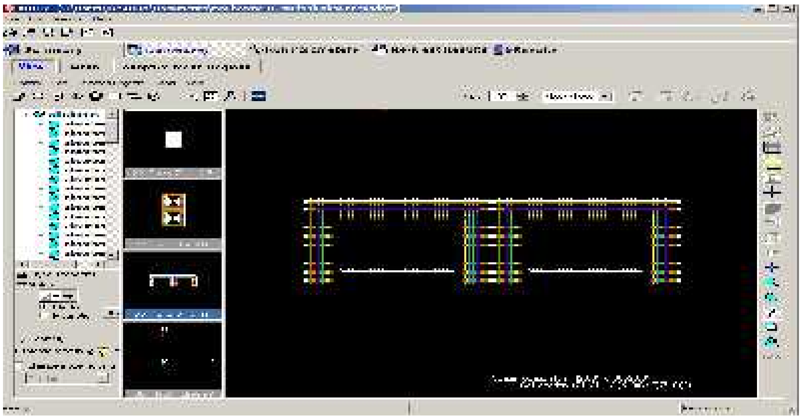

Figure (5-28) xfdtd Geometry of Two Bowtie Antennas to Work as GPR System

First simulation of GPR system was done in free space, second over dry sand ($\sigma = 10^{-5}$, $\varepsilon_r = 2.3$) without any buried target, third simulation over dry sand in presence of target (metal mine) and the last simulation over dry sand with target (plastic casing mine) as shown in Figure (5-29).

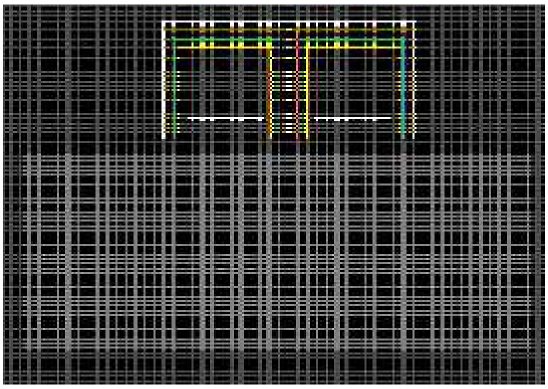

(a)

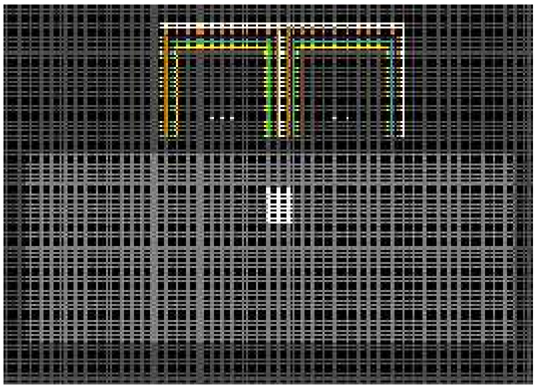

(b)

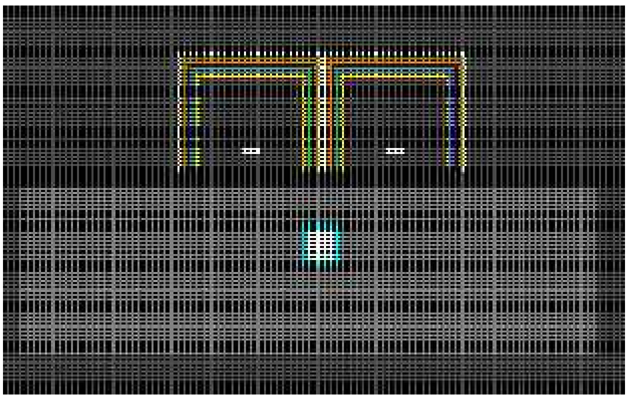

(c)

Figure (5-29) xfdtd Geometry of GPR System Over Dry Sand (a) without Target (b) with Target (Metal Mine) (c) with Target (Plastic Casing Mine)

Figure (5-30) shows the magnitude of transmission coefficient S_{21} between transmitting antenna and receiving antenna of GPR system. By comparing magnitude of S_{21} in case of GPR system over dry sand ($\sigma = 10^{-5}$, $\varepsilon_r = 2.3$) without target as shown in Figure (5-30.a) with that's in case of GPR system over dry sand with target (metal mine) as shown in Figure (5-30.b), it's clear the change in transmission coefficient $|S_{21}|$ which is an indication of presence of a target. In case of plastic casing mine, change $|S_{21}|$ is small compared with ones of metal target as shown in Figure (5-30.c).

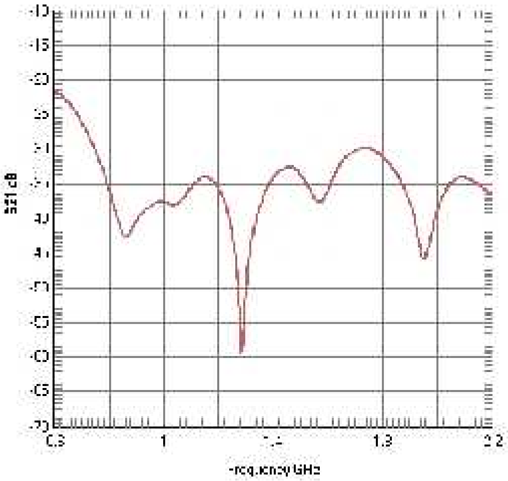

(a)

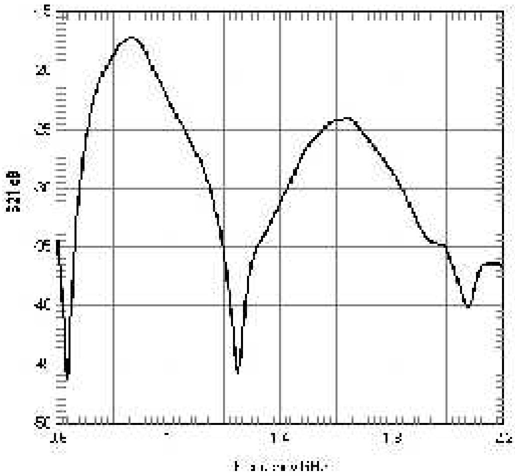

(b)

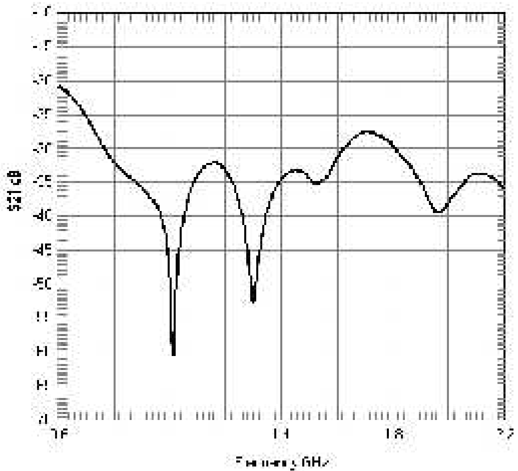

Figure (5-30) $|S_{21}|$ vs. Frequency of GPR System Over Dry Sand (a) without Target (b) with Target (Metal Mine) (c) with Target (Plastic Casing Mine)

Chapter 6

Using Vector Network Analyzer (VNA) with Horn Antenna to Work as a GPR System

6-1 Introduction

Vector network analyzer VNA is a general-purpose laboratory equipment has a wide operating frequency range and other controllable parameters to cover a certain bandwidth. The frequency step size can be changed through the available control features of the vector network analyzer. In this part of thesis we have used two horn antennas connected to VNA as shown in Figure (6-1), to work as GPR system to examine presence of some objects buried under surface of ground (two different soils and clay).

VNA measures the magnitude and phase characteristics, these can be used to measure target parameters in the frequency domain and in the time domain **[26]**.

Figure (6-1) VNA Connected with Two Horn Antennas

In this part of thesis we tried to check the performance of GPR system (VNA connected with horn antenna) over three types of soils, estimating the velocity of EM wave in sand soil, dielectric constant of clay soil and try to detect metal targets in both soils by measuring the transmission coefficient S_{21} between two antennas.

6.2 EM Wave Velocity Through Sand Soil

Electromagnetic wave velocity v in dielectric medium is governed by the relative permittivity (dielectric constant ε_r of medium) and by relative permeability μ_r.

$$v = \frac{c}{\sqrt{\varepsilon_r \mu_r}} \qquad (6\text{-}1)$$

For Non-magnetic materials (i.e., most rocks and soils) the value of $\mu \simeq \mu_\circ$, hence their relative permeability μ_r is approximately equal to one.

Then equation (6-1) becomes

$$v \cong \frac{c}{\sqrt{\varepsilon_r}} \qquad (6\text{-}2)$$

Experiment 1:GPR system over a sand **(**$\varepsilon_r = 2.3$**)**

The setup of experiment is as shown in Figure (6-2) below:

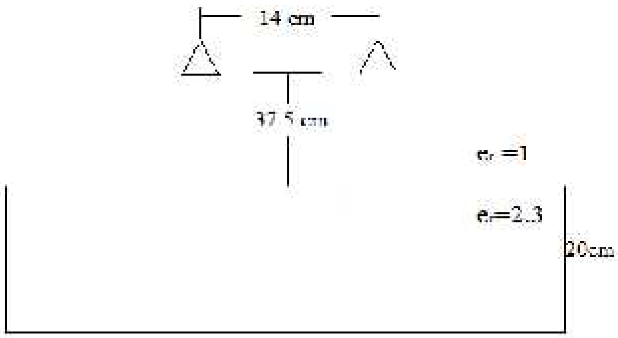

Figure (6-2) Setup of Experiment (1)

-distance between two antennas **14 cm**.
-distance from midpoint between two horns to upper surface of sand about **37.5cm**.
-dimensions of soil box (long=**80 cm**, width=**80 cm** and height=**20 cm**).
-soil dielectric constant $\varepsilon_r = 2.3$

From the graph of transmission coefficient S_{21} versus time as shown in Figure (6-3), it is noticed that the two clear pluses appear after we remove the direct leakage signal between the antennas, the first at the time (**3.77 ns**) which involved of the upper surface of the sand, the second appear at the time (**5.82 ns**) which involved of the bottom surface of the sand.

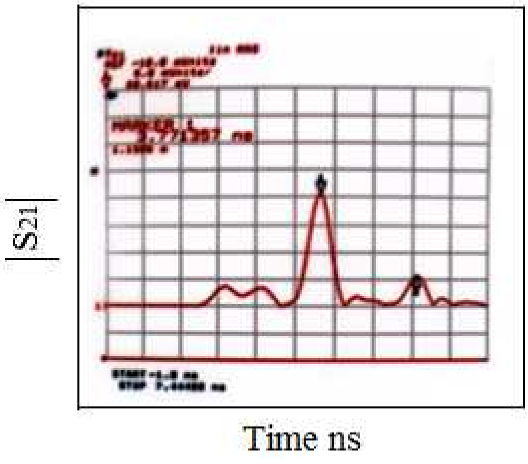

Figure (6-3) S_{21} Magnitude vs. Time

By using triangulation to approve the above results

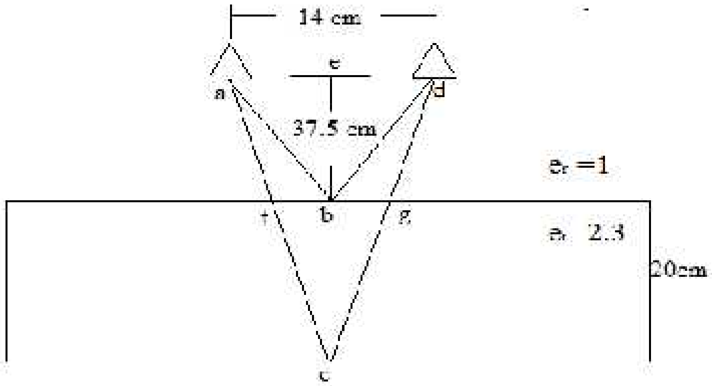

Figure (6-4) Experiment (1) Calculation Sketch

1- first pulse at 3.77 n sec

From Figure (6-4), the distance from *a* to *b* (path from Tx antenna to upper surface of soil) equal to:

$ab = \surd[(e\ )^2+(eb)^2\ ] = \sqrt{(7^2+37.5^2)} = 38.15$ cm

then the path from Tx horn ***a*** to soil upper surface ***b*** to Rx horn ***d*** is:

ab+bd =38.19*2= 76.30 cm.

by using the relation

$$d=c*t \quad (6\text{-}3)$$

where c ≡ speed of EM wave in free space = $3*10^8$ m/sec

t ≡ two way travel time in seconds

d ≡ path distance in meters

note: there is a delay in antennas about 1.25 n sec **[25]**

The two way traveling time (TWTT) = $0.763/3*10^8$ =2.54 n sec

By adding time delay at antennas

TWTT = 2.54 + 1.25 = 3.79 n sec, which is nearly equal the time of the first pulse (reflection from upper surface).

2- second pulse at 5.82 n sec

It is expect that this pulse reflection is from the bottom surface of sand soil, so the wave path consists of path in free space and another in sand soil, hence it can determine the velocity of EM wave in sand soil from Figure 6-4, the distance from *a* to *c* (path from antenna to bottom surface of soil) equal to:

$a\text{-}c = \surd[(e\ )^2+(ebc)^2\ ] = \sqrt{(7^2+57.5^2)} = 57.9$ cm

Distance *f -b* = 7 x 20/57.5 =2.45 cm

Then path f- $c = \sqrt{(20^2 + 2.45^2)} = 20.15$ cm

Total path through sand soil is: $fc + fg = d_2$ = 20.15+20.15 = 40.3 cm

Total path through free space: $af + gd = d_1$ =37.75 + 37.75 = 75.5 cm

So the TWTT is:

TWTT = $\frac{d_1}{c} + \frac{d_2}{v} = \frac{0.7}{3*10^8} + \frac{0.4}{v}$ = (5.82 - 1.25) *10^{-9} sec

v =1.97*10^8 m/sec

Which is about the same as if we use the equation (6-2)

$$v \cong \frac{c}{\sqrt{\epsilon_r}} = \frac{3*10^8}{\sqrt{2.3}} = 1.978*10^8 \text{ m/sec}$$

6-3 Estimation of Dielectric Constant of Clay Soil

As it has mentioned in chapter two, electromagnetic wave propagation in dielectric materials is governed by electrical properties of those materials such as permittivity, conductivity and permeability.

Thus, in the next experiment we try to estimate the dielectric constant ϵ_r of clay soil by measuring the delay time.

Experiment (2):GPR system over a clay soil (ϵ_r = **?**)

-distance between two antennas 14 cm

-distance from horn to upper surface of sand 31cm

-volume of sand container (length=80 cm, width=80 cm and height=16.5 cm).

The arrangements of experiment as in Figure (6-5) below:

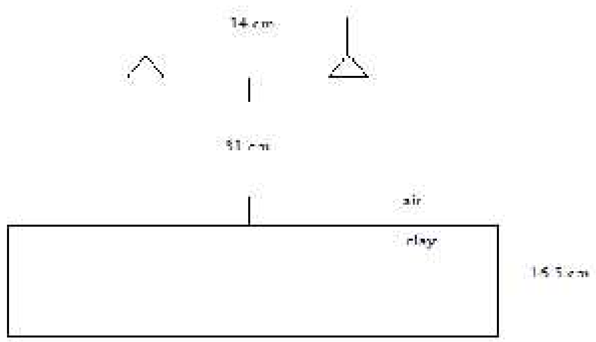

Figure (6-5) Setup of Experiment (2)

The four clear pluses appear as shown in Figure (6-6), the first and the second are from the leakage between two antennas, the third at the time (3.371 ns) which involved of the upper surface of the clay, the fourth appear at the time (5.389 ns) which involved of the bottom surface of the clay.

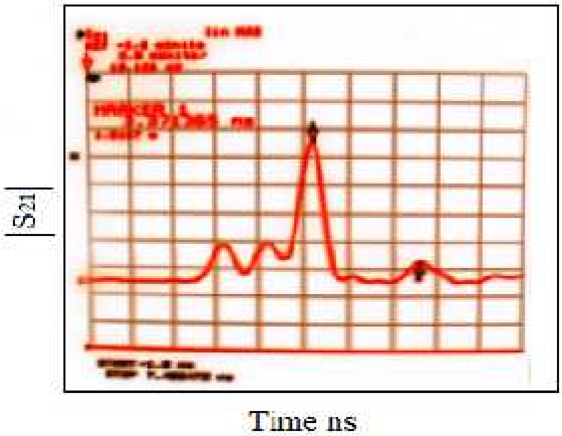

Figure (6-6) $\mathbf{S_{21}}$ Magnitude vs. Time (ns) of Experiment (2)

In this experiment, the dielectric constant of clay was unknown, so we will try to estimate it by using TWTT (time of fourth pulse = 5.389 n sec)

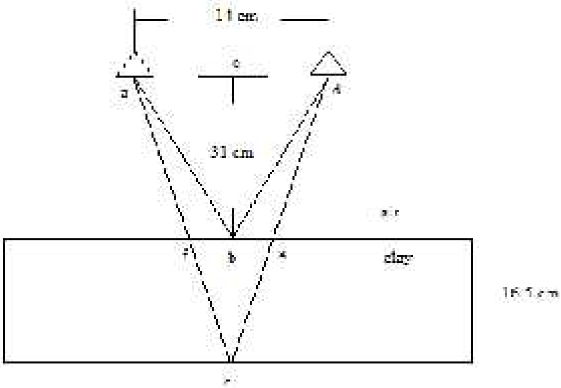

Figure (6-7) Experiment (2) Calculation Sketch

From Figure (6-7) it can be determine:

Path of signal in free space *a-f* plus *g-d* = 31.32 + 31.32 = 62.64 cm

Path of signal in clay *f-c* plus *c-g* = 16.68+16.68 = 33.36 cm

TWTT in overall path = $\frac{C.6}{3*1\ 8} + \frac{0.3\ \sqrt{\epsilon_r}}{3*1\ 8}$ =(5.389 $*10^{-9}$ -1.25$*10^{-9}$)sec

2.088 + 1.112 $\sqrt{\epsilon_r}$ = 4.139 → $\sqrt{\epsilon_r} = \frac{4.1 \quad -2.0}{1.1}$

$\epsilon_r = 3.4$

6-4 Detection of Buried Metal Targets into Different Soils

The basic principle of GPR system to detect objects beneath the ground surface is that the transmitting pulse reflects when hits a boundary where there is an abrupt change in dielectric constant, the range is proportional to the time difference from transmission to reception of the echo, so the range can be determined using time difference and the knowledge of the dielectric constant of the medium **[27].**

Experiment (3):GPR system over a sand ($\varepsilon_r = 2.3$) with metal target

-distance between two antennas 14 cm

-distance from horn to upper surface of sand 36.5cm.

- dimensions of sand box (long=80cm, width=80 cm and height=20 cm).

-metal target at distance 8.5 cm under the sand surface.

-metal target dimensions (diameter =6.5 cm, height =2.7cm)

The arrangements of experiment as in Figure (6-8) below:

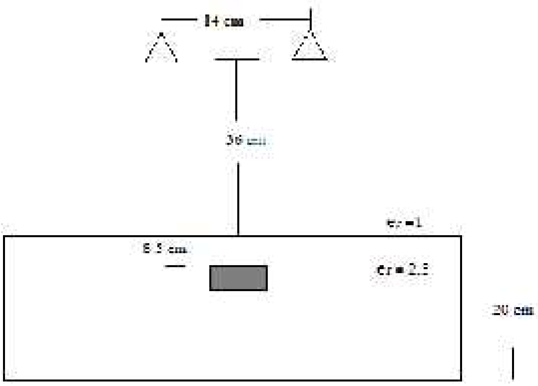

Figure (6-8) Setup of Experiment (3)

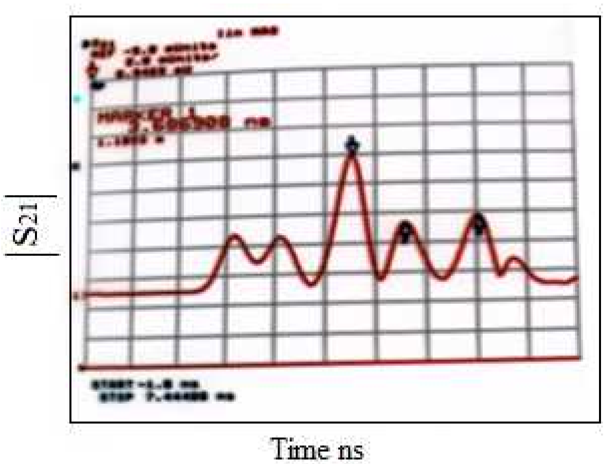

Figure (6-9) $\mathbf{S_{21}}$ Magnitude vs. Time (ns) of Experiment (3)

From Figure (6-9) group of pluses appear, the first and the second from the leakage between two antennas, the third at the time (3.686 ns) which involved the upper surface of the sand, the fourth appears at the time (4.57 ns) which involved the metal target, the fifth pulse appears at the time (5.798 ns) which involved the bottom surface of the sand .

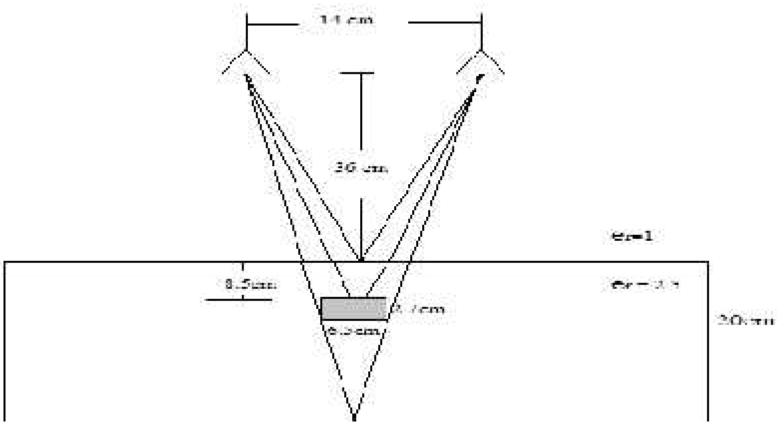

Figure (6-10) Experiment (3) Calculation Sketch

By using the same manner (triangulation) as in experiment (1) and from Figure (6-10), it can determine TWTT of the reflections as follows:

a- Reflected pulse at time (3.68 n sec)

Path from antenna to upper surface = $\sqrt{(7^2+36^2)}$ = 36.67 cm

Then the overall path (from Tx antenna to Rx antenna) = 73.34cm

TWTT =$[0.7334/(3*10^8)]+1.25 *10^{-9}$ = <u>3.695 n sec</u>

b- Pulse at time (4.57 n sec)

Path from antenna to metal target = $\sqrt{(7^2+44.5^2)}$ = 45 cm

Which consists of, path in free space and path in soil

Path in free space =2*(45 - 8.6) = 72.8 cm

Path in soil = 2*(8.6) = 17.2 cm

TWTT in overall path $= \frac{0.7}{3*1\ \ 8} + \frac{0.1\ \ \sqrt{2.3}}{3*1\ \ 8} = 3.296 *10^{-9}$ sec

TWTT + delay in ant = 3.296 n sec + 1.25 n sec = 4.55 n sec nearly equal time of fourth pulse.

c- Reflected pulse at time (5.79 n sec)

Path from antenna to bottom surface = $\sqrt{(7^2+56^2)}$ = 56.4 cm

Which consists of path in free space and path in soil

Path in free space =2*(56.4 – 20.16) = 72.48 cm

Path in soil = 2*(20.16) = 40.32 cm

TWTT in overall path $= \frac{0.7}{3*10^{8}} + \frac{0.4\ \sqrt{2.2}}{3*10^{8}} = 4.45*10^{-9}$ sec

TWTT + delay in ant = 4.45 n sec + 1.25 n sec = 5.8 n sec nearly equal time of fifth pulse.

Experiment (4):GPR system over a clay soil in presence of metal target

-distance between two antennas 14 cm.

-distance from horn to upper surface of clay soil 32cm.

-volume of sand container (length=80 cm, width=80 cm and height=16.5 cm).

-target at distance 5.5 cm under the clay soil surface

-target dimensions (diameter =6.5 cm, height =2.7cm)

Figure (6-11) shows the setup of experiment (4).

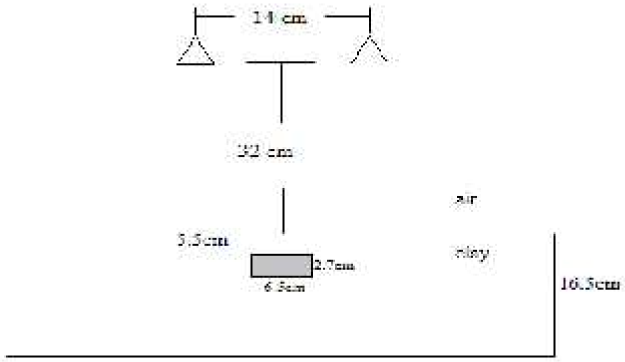

Figure (6-11) Setup of Experiment (4)

Referring to Figure (6-12), two clear pluses appear (marked), the first at the time (3.436058 ns) which is from the upper surface of the clay soil, the second appear at the time (4.129849 ns)) from the target.

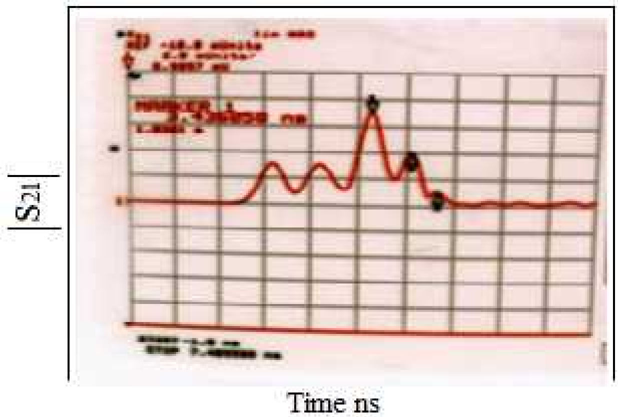

Figure (6-12) S_{21} Magnitude vs. Time (ns) of Experiment (4)

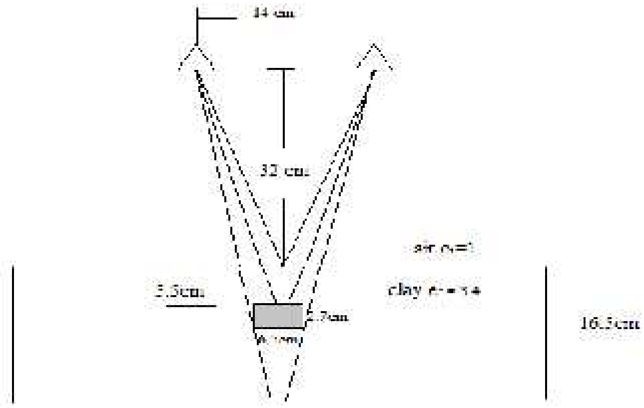

Figure (6-13) Experiment (4) Calculation Sketch

From Calculation Sketch shown in Figure (6-13) it can be determine the follows:

Path from Tx antenna to upper surface to Rx antenna equal to:

32.76 + 32.76 = 65.52 cm

TWT of this path = 0.6552/(3*10^8) = 2.184 n sec

2.184 + 1.25 = 3.434 n sec which is nearly equal the time of first marked pulse .

Path from Tx antenna to upper surface of target to Rx antenna equal to:

free space path = 2*(38.15 – 5.6) =2* 32.55 = 65.10 cm

clay soil path = 2*5.6 = 11.2 cm

TWTT in overall path $= \frac{0.6}{3*1\ \ 8} + \frac{0.1\ \ \sqrt{3.4}}{3*1\ \ 8}$ = 2.858 n sec

TWTT + delay in ant = 2.858 n sec + 1.25 n sec = 4.108 n sec which is nearly equal the time of second marked pulse.

We note the last pulse at time (4.59 n sec) is very small, may be because the clay soil has high attenuation and the signal take a long path.

6-5 Effect of Antenna Bandwidth on Range Resolution

GPR range resolution is the ability of the radar to distinguish two targets with similar ranges. The resolution is determined by the signal bandwidth, BW. The smallest time interval that the radar can resolve is the inverse of the bandwidth **[28]**:

$\tau = 1 / BW$ (6-4)

which gives a range resolution ΔR of:

$\Delta R = \frac{c\,\Delta\tau}{2}$ = c/(2BW) (6-5)

where c is the signal velocity (3*10^8 m/s in air).

Experiment (5) ***GPR system over sand soil (ε_r =2.049)***

In this experiment next we used GPR system over sand soil to show the effect of antenna bandwidth on range resolution.

The arrangement of experiment as shown in Figure (6-14) .

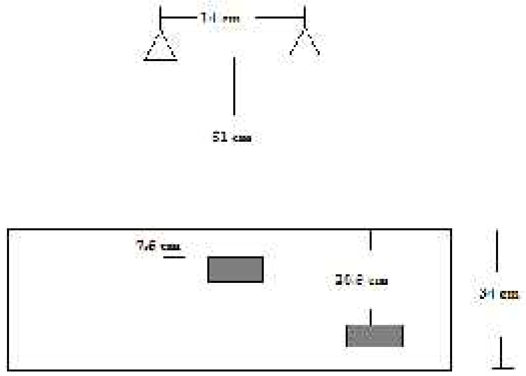

Figure (6-14) Setup of Experiment (5)

-Distance between two antennas is 14 cm

-Distance from horn to upper surface of soil 51cm

-Dimensions of sand soil box (80 cm x 80 cm x 34 cm)

-Two targets at distances 7.5 cm and 26.5 cm under the soil surface

-Metal target dimensions (diameter =6.5 cm, height =2.7cm)

a)- bandwidth of the antennas 4 GHz (3.6-7.6 GHz)

From the Figure (6-15) we have noticed a group of pluses, the first and the second from the leakage between two antennas at the times (1.783 n sec &2.818 n sec respectively), the third at the time (4.589 n sec) which is from the upper surface of the sand soil, the fourth appears at the time (5.44 ns) which is estimated to be from the upper target, the fifth pulse appears at the time (7.096 n sec) which is estimated to be from the lower target and last reflection appears at the time (7.648 n sec) which is from the bottom surface of the sand soil.

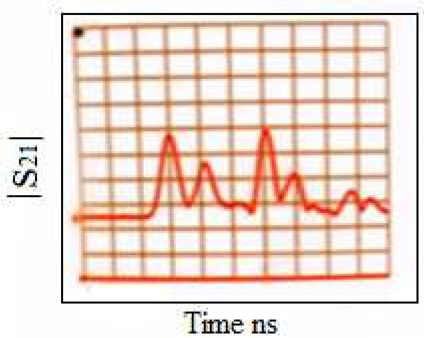

Figure (6-15) $\mathbf{S_{21}}$ Magnitude vs. Time (ns) of Experiment (5)

We have noticed from Figure (6-15), that the pulses are clear and can be distinguish from each other which is due to the adequate system bandwidth 4 GHz.

b)- bandwidth of the antennas 2 GHz (4.6 - 6.6 GHz)

By using the same arrangements above as in Figure (6-15) and change the frequency range of antennas from *(3.6 - 7.6 GHz)* to *(4.6 - 6.6 GHz)* i.e. BW = 2 GHz.

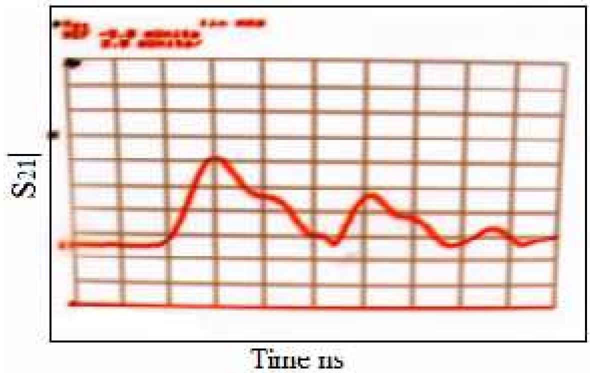

Figure (6-16) $\mathbf{S_{21}}$ Magnitude vs. Time (ns) of Experiment (5) BW of 2 GHz (4.6 - 6.6 GHz)

From Figure (6-16), it's clear that the pluses are overlap and they cannot be distinguish from each other, which is due to the decreasing of bandwidth.

c) -bandwidth of the antennas 1 GHz (4.5 - 5.5 GHz)

By decreasing system bandwidth to *1 GHz (4.5 - 5.5 GHz)* the pulses become more overlapped as shown in Figure (6-17).

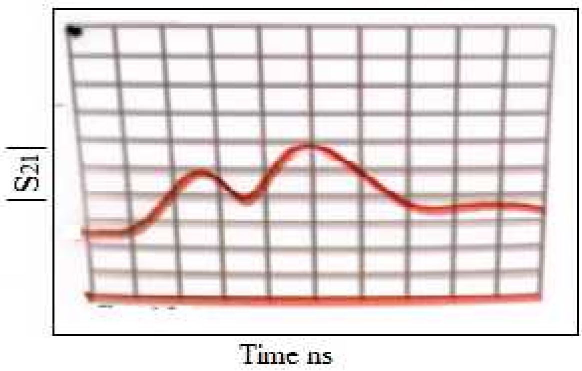

Figure (6-17) $\mathbf{S_{21}}$ Magnitude vs. Time (ns) of Experiment (5) BW of 1 GHz (4.5 - 5.5 GHz)

6-6 Effect of Increase of Central Frequency on Target Detection

Ground acts like a low pass filter which attenuates the higher frequencies i.e. lead to low depth of penetration, the ground is a lossy medium with attenuation ranging from 10 dB/m at 3 to 300 MHz to 100s of dB/m at GHz frequencies **[25]**.

In this experiment we will use the same antennas which were used in the all previous experiments BW= 4 GHz (3.6-7.6 GHz) f_o =5 GHz, but for next experiments we will use antennas of frequency range (12 - 18 GHz) and changing a center frequency (14, 15 and 16 GHz) to show the effect of increasing the central frequency with keeping BW of 4 GHz.

Experiment (6)   BW= 4 GHz (3.6-7.6 GHz) f_o =5 GHz

The arrangements of experiment as in Figure (6-18) below:

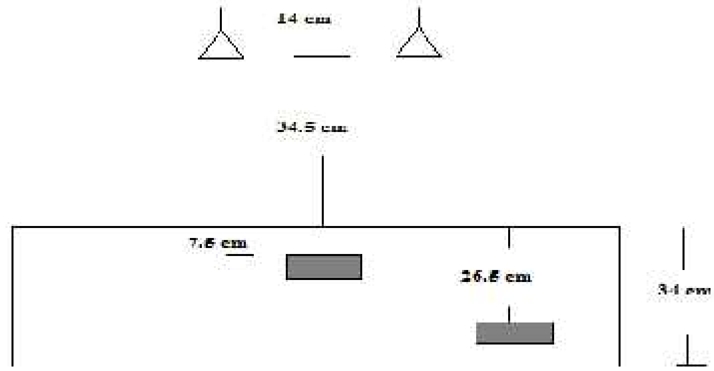

Figure (6-18) Setup of Experiment (6)

Figure (6-18) shows a group of pluses, first at the time (3.575 ns) which is from the upper surface of the soil, the second appear at the time (4.375 ns) which estimated from the upper metal target.

The third pulse appears at the time (6.1 ns) which is from lower target and last reflection appear at the time (6.825 ns) which is from bottom surface of sand soil.

At central frequency f_0=5 GHz and BW=4GHz we could estimate the ranges of reflections as shown in Figure (6-19.a), i.e. good resolution and sufficient depth of penetration. Therefore, when we increase frequency band to 12- 18 GHz with f_o = 15 GHz, the depth of penetration will be low, due to the attenuation for high frequencies as shown in Figures (6-19.b), (6-19.c) and (6-19.d), so the wave cannot reach the deeper targets (lower metal target and bottom surface of sand soil).

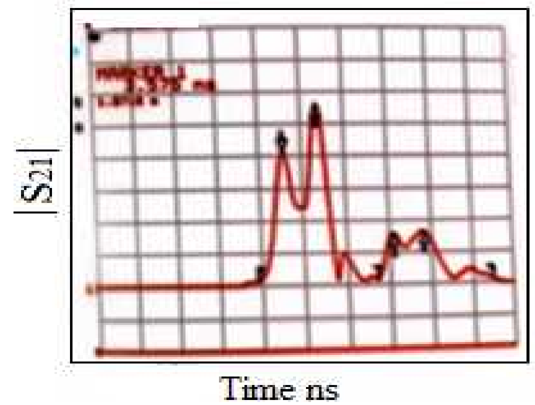

a) BW= 4 GHz (3.6-7.6 GHz) f_o =5 GHz

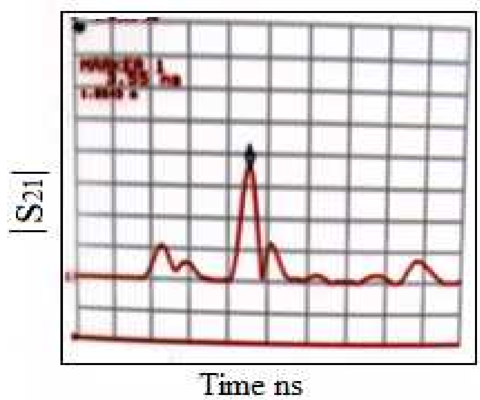

b) BW=4GHz (12-16 GHz) f_o = 14GHz

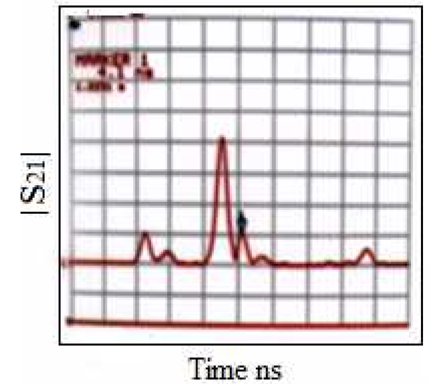

c) BW=6GHz (12-18 GHz) f_o = 15GHz

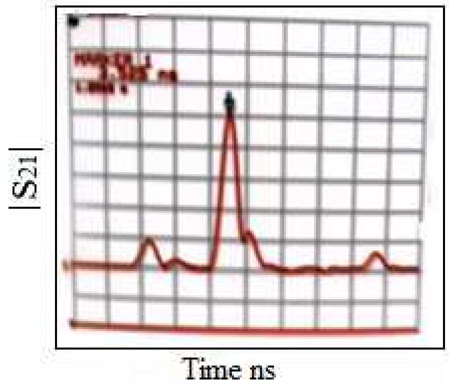

d) BW=4GHz (14-18 GHz) f_o = 16GHz

Figure (6-19) $\mathbf{S_{21}}$ Magnitude vs. Time (ns) of Experiment (6)

Chapter 7

Conclusion and Future Work

7-1 Conclusions

In this dissertation, the work done is divided into two parts; part one was in optimizing and simulating the bowtie antenna for GPR in field of landmines detection by using FDTD method and part two was using a VNA with two horn antennas to work as a GPR system to test effect of ground and radar signal frequency and bandwidth on the capability of the radar to detect landmines.

The main objective of part one was to model and simulate a single GPR antenna and optimize this antenna to obtain a good performance to achieve GPR requirements for landmines detection (low antenna ringing, wide bandwidth and directive pattern).

Firstly, bowtie antenna is simulated in free space according to source impedance of 50 ohm, it is found that the antenna has a narrow bandwidth about 120 MHz, but when matching circuit is used, the antenna presented a wide bandwidth about of 570 MHz .

Second simulation was by loading bowtie antenna with resistive load to reduce the time late ringing (or antenna ringing), the results presented a quiet good decrease in time-late ringing but with slightly decrease in antenna gain.

A copper shield was used to cover bowtie antenna to concentrate most of radiation into ground, three heights of copper shield is used (5cm, 10 cm and 15 cm) in presence of resistive loading, the results presented that the bowtie antenna with 10cm shield height has better frequency response than others (i.e. bandwidth of 870 MHz, low ringing and reasonable radiation pattern).

To obtain more improvements for bowtie antenna characteristics over a wide frequency band, the inner walls of copper shield were padded by layers of gradually conductivity profile to act as electromagnetic absorbers that help absorb unwanted radiation in the upper half space.

Results have shown that the bowtie antenna with padded copper shield has quite good characteristics; antenna bandwidth has improved to reach to about 1.65 GHz, which is one important requirement for GPR antenna.

Also antenna with padded copper shield has a slightly lower ringing than the antenna with copper shield only and has more desirable radiation pattern than without it i.e. the padding has concentrated the radiation pattern in one direction.

Another simulation was done to study the effect of ground on bowtie antenna characteristics, two types of soils was modeled, dry sand soil *(low losses ground)* with electrical properties ($\sigma = 10^{-5}$, $\varepsilon_r = 2.3$) and clay soil *(lossy ground)* with electrical properties ($\sigma = 10^{-1}$, $\varepsilon_r = 6$) and the antenna placed at two positions, touching ground surface and 5 cm above ground surface. Results from the case of dry sand soil have shown that ground has deteriorating effect on bowtie antenna characteristics especially when antenna is placed directly on the ground surface, hence keeping the antenna slightly above ground is better.

In case of clay soil also results have shown that the clay has worse effect on bowtie antenna characteristics than that of dry sand.

Last simulation done was in examination of two bowtie antennas to work as GPR system, one antenna for transmitting and another for receiving.

The capability of the GPR system to detect buried targets can be measured from the change in coupling coefficient $|S_{2}|$ between the transmitting antenna and the receiving antenna.

The simulations was done over a dry sand ($\sigma = 10^{-5}$, $\varepsilon_r = 2.3$) without any buried target, in presence of target (metal mine) and the last simulation was over a dry sand with target (plastic casing mine).

By comparing magnitude of S_{2} in case of GPR system over dry sand without target with that in the case of GPR system over dry sand with target (metal mine), it is clear the change in transmission coefficient $|S_{2}|$ which is an indication of presence of target. In case of plastic casing mine, there is a change in $|S_{2}|$ but it is small compared with case of metal target.

In part two of this thesis two horn antennas were connected with VNA to be used as a GPR system. The performance of GPR system is studied over three types of soils, the velocity of EM wave in sand soil is estimated, also dielectric constant of clay soil and a trial to detect metal targets in both soils by measuring the transmission coefficient S_{21} between two antennas was done.

The effect of bandwidth on target resolution is studied in three cases of bandwidth (1 GHz, 2 GHz and 4 GHz) and proved that the resolution increases by increasing bandwidth.

Also effect the change of central frequency on depth of penetration i.e. in target detection is studied in cases of central frequency of (5, 14, 15 and 16 GHz) and proved that the high frequency leads to low depth of penetration i.e. limits target detection.

Therefore, GPR antenna design must make a trade-off between quality of the image, (i.e. large bandwidth) and required penetration depth. Which mainly depended on type of application, in case of landmine detection, we need larger bandwidth more than it needs large penetration depth because most of land mines are placed close to the surface of the earth.

7-2 Future Work

Future work can to be done in signal processing techniques to calculate the Inverse Fourier Transform and providing the phase of the transmission coefficients S_{21} to obtain the signal in the time domain. From time domain results of reflections the range of the target is estimated.

An investigation can be done on new and promising antenna design concepts such as “Fractal Antennas” that minimize the antenna size and at the same time increase the directivity **[29]**.

References

[1] A. M. Zoubir, Ian James Chant, Christopher L. Brown, Member, IEEE, Braham Barkat, and Canicious Abeynayake, "**Signal Processing Techniques for Landmine Detection Using Impulse GPR**", IEEE Sensor Journal, 2002.

[2] Joynt, V.P., "**Mobile Metal Detection: a Field Perspective**", Proceedings of the Second International Conference on the Detection of Abandoned Land Mines, Edinburgh, UK, pp. (14-15) 1998.

[3] **Landmines**, United Nations Office For Disarmament Affairs http://www.un.org/disarmament/convarms/landmines/ 2011.

[4] MacDonald et al**. "Innovative Mine Detection Systems"** (chapter 4) Rand, Santa Monica, CA, 2003.

[5] P. Mächler **"Detection Technologies for Anti-Personnel Mines"** Symposium on Autonomous Vehicles in Mine Countermeasures, Monterey, April 1995.

[6] DOD's Research Program Needs a Comprehensive Evaluation Strategy "**LAND MINE DETECTION"** http://www.globalsecurity.org 2001.

[7] Alauddin Bhuiyan and Baikunth Nath **Anti-Personnel Landmine Detection Based on GPR and IR Imaging**: A Review Computer Science and Software Engineering, The University of Melbourne, Melbourne, Australia, 2010.

[8] Ning Xiang1 and James M. Sabatier **"Applications of Acoustic-to-Seismic Coupling for Landmine Detection"** 2002.

[9] J.C. Kapoor and G.K. Kannan **Landmine Detection Technologies to Trace Explosive Vapour Detection Techniques** Defense Science Journal, Vol. 57, No. 6, November 2007.

[10] Maki K. Habib **"Bio-Inspiration and Mine Detection"** Mechanical Engineering Department, School of Sciences and Engineering, American University in Cairo, Egypt, 2012.

[11] C. P. Gooneratne, S. C. Mukhopahyay and G. Sen Gupta "**A Review of Sensing Technologies for Landmine Detection: Unmanned Vehicle Based Approach"** 2nd International Conference on Autonomous Robots and Agents December 13-15, 2004 .

[12] D. J. Daniels, " **Ground Penetrating Radar**," The Institution of Electrical Engineers,(IEE) London, United Kingdom 2004.

[13] Wamweya, Amos "**Application Of Ground Penetrating Radar (GPR) For Bridge Deck Condition Assessment: Using a 1.5 GHz Ground- Coupled Antenna"** Missouri University of Science and Technology 2009.

[14] Roberto N. Barbosa and C. Overstreet **"What Is Soil Electrical Conductivity?"** www.LSUAgCenter.com, 2011.

[15] G.Topp, J. Davis, A.P. Annan, "**Electromagnetic Determination of Soil Water Content: Measurements in Coaxial Transmission Lines,**" Water Resources Research, vol. 16, pp. 574-582, 1980 .

[16] Constantine A. Balanis **"Antenna Theory Analysis And Design"** Published by John Wiley & Sons, Inc., Hoboken, New Jersey. Third Edition 2005.

[17] R. Clarke, R. Karunaratni, C. Schrader, "**Ultra-Wide Band Antenna**", College of Engineering, San Jose State University. Fall 2004.

[18] Disala Uduwawala **"A Comprehensive Study of Resistor-Loaded Planar Dipole Antennas for Ground Penetrating Radar Applications"** Doctoral Thesis Division of Electromagnetic Engineering School of Electrical Engineering Royal Institute of Technology Stockholm, Sweden 2006.

[19] M. S. Jayakumar **"Antenna Optimization For Ground Penetrating Radar Using The Finite Difference Time Domain Technique"** master thesis**,** South Dakota School Of Mines And Technology Rapid City, South Dakota 1999.

[20] A.A. Lestari, A.G. Yarovoy, L.P. Ligthart, "**An efficient Ultra-Wideband Bowtie Antenna**" *Proceeding European Microwave Conference*, London, UK, pp. 120-132, September 2001.

[21] Remcom XFDTD version 6.3 **Three-dimensional Full Wave Electromagnetic Analysis Software** reference manual, 2001.

[22] Remcom XFDTD version 6.3 **Three-dimensional Full Wave Electromagnetic Analysis Software** user guide, 2001.

[23] G. E. Atteia, A. A. Shaalan and K. F. A. Hussein "**Wideband Partially -Covered Bowtie Antenna For Ground–Penetrating Radars**" Progress In Electromagnetics Research, PIER 71, 211–226, 2007.

[24] **RF Tools, LC Impedance Matching Network Designer Software** http://www.leleivre.com/rf_lcmatch.html 1999.

[25] Omar S. Elshebani, S. I. Elkhetali, K. S. Belgath **"Utilizing the Vector Network Analyzer To Work as a GPR for Detection of Hidden Objects"** R & D center 2006**.**

[26] **Agilent Technologies 8510C Network Analyzer System** Operating and Programming Manual, 2001.

[27] Simon Kingsley and Shaun Quegan "**Understanding Radar Systems**" SciTech publishing inc. first Indian edition 2001.

[28] C. F. Hu, and L. X. Zhang **"Indoors Accurate RCS Measurement Technique On UHF Band"** UAV Specialty Technique Key Laboratory of National Defense Technology Northwestern Polytechnic University 2008**.**
[29] John D. Kraus and R.J. Marhefka **"Antennas For All Applications**" McGraw-Hill Higher Education Third Edition 2002.